SunPower® Module Degradation Rate

Summary

Section I provides a detailed design comparison showing that the integrated back contact design of SunPower Maxeon® solar cells makes them inherently more robust than conventional cells in real-world conditions. Standard accelerated testing shows that they are almost impervious to the dominant failure modes (moisture, thermal cycling, and mechanical loading) that degrade conventional cells.

In Section II, fundamental reliability physics research is reviewed. SunPower has identified key degradation modes which have been rigorously studied and modeled. Individual degradation mechanisms have been validated with accelerated laboratory testing and field monitoring. This effort has led to the development of PVLife, a multi-stress fully-coupled thermal-electrical dynamic model of module performance, degradation and failure. The results of this model are compared to a recent fleet-wide degradation study and the details are discussed, with references to recently-published articles in industry conference proceedings for additional detail. Using PVLife, SunPower is able to predict, with a high degree of confidence, the degradation rate and failure probability of SunPower modules and systems.

Section III describes how SunPower continues to enhancing the reliability of its modules via systematic advances addressing each major degradation and failure mode. SunPower's current generation of modules is compared it to the previous generation in numerous side-by-side accelerated tests. Several key degradation stresses are applied, showing that SunPower's current generation is indeed even more reliable, and is expected to have an even lower degradation rate. SunPower's physics model, when incorporating lab results from these accelerated tests, predicts a system degradation rate of 0.17% per year ± 0.12% per year in a typical hot/dry climate power-plant application at 90% confidence. This represents the highest degradation environment.

Specific conclusions of this report are:

- The Maxeon cell design is fundamentally more robust against real-world stresses, resulting in modules that have fewer failure modes and degrade at a lower rate than Conventional Modules[1].
- SunPower has conducted years of fundamental research and can accurately predict module degradation rates using PVLife.
- An average system degradation rate of <0.25% per year for SunPower's current technology accounts for different climates and deployment conditions.

[1] A Conventional Module is defined as 240W, 15% efficient, approximately 1.6 m^2

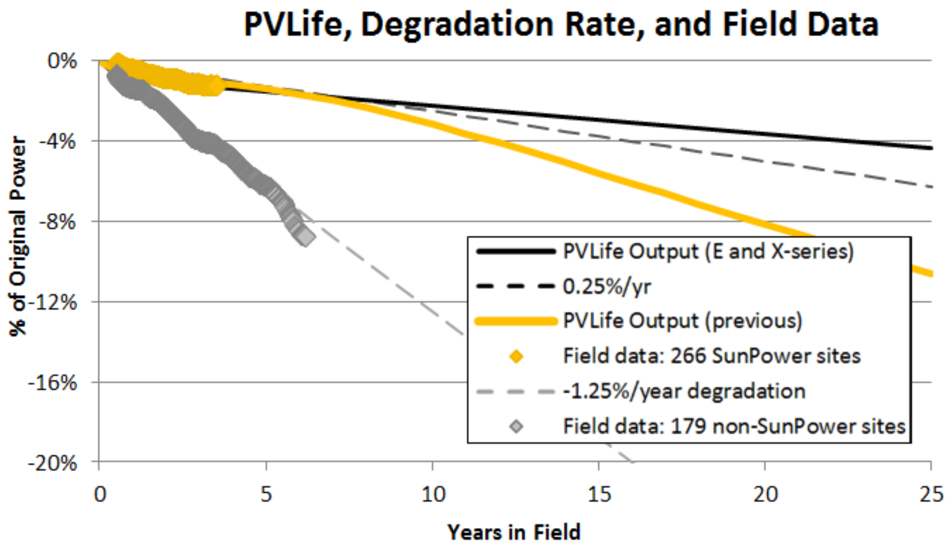

Figure 1: Actual field data compared to SunPower's physics-based degradation model, PVLife. PVLife modeling shows the current generation of SunPower modules exhibit 60% less degradation, a rate of less than 0.25% per year.

Contents

Part I: Real world stresses and the SunPower Reliability Advantage

Introduction

PV has become an increasingly reliable technology thanks to long-term investment by numerous research organizations and governments. For example, a series of five "block buys" were conducted by NASA's Jet Propulsion Laboratory from 1975-1981, each with successively more stringent qualification criteria, resulting in early failure rate reduction from 45% in Block I, to 0.1% in Block V. Significant efforts by the Joint Research Center of the European Commission [1], and adaptation of accelerated stress tests originating from the semiconductor industry, such as damp heat [2], have also contributed substantially. A key theme in these studies has been that failure rates are generally lower when modules pass more stringent tests. Understanding how module manufacturers qualify their materials is a strong indicator for long term reliability.

These efforts ultimately resulted in the creation of certification standards, tests a module must pass in order to be sold. Examples include IEC61215 and U1703. However, many manufacturers assume that this *certification* testing is sufficient for *qualification*; however, the goal of these tests is not to determine lifetime reliability, rather, it is to identify short-term issues [3] [4]. In other words, certification tests are designed to ensure a nominal level of safety and design quality, and not to indicate whether or not a product will last for its warranted lifetime. Despite this, many module manufacturers continue to struggle to meet these basic requirements (Figure 2).

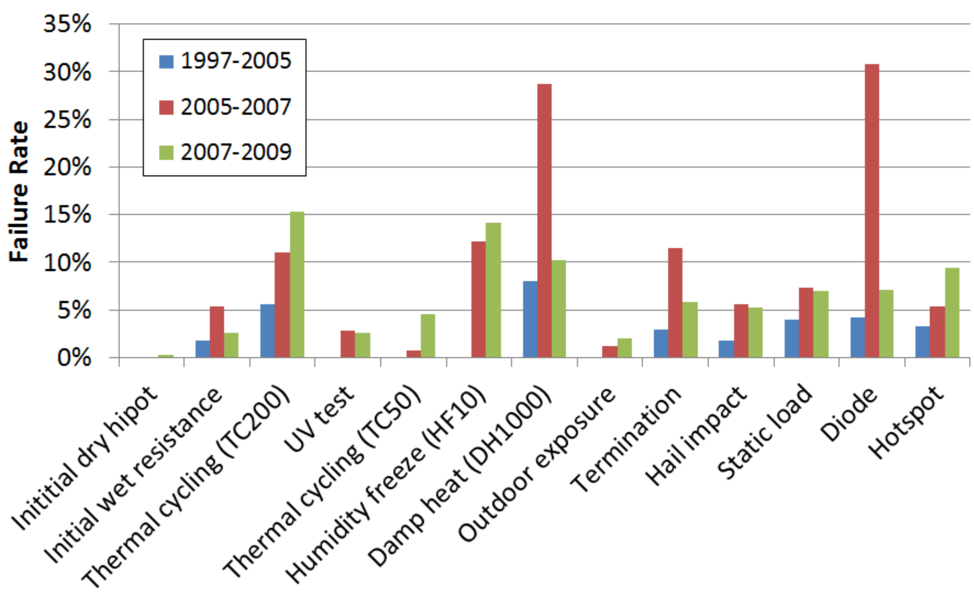

Figure 2: Certification test failure rate for c-Si modules. Each color corresponds to a different range of production years. Despite increasing capacity over the sample years, products continue to fail basic certification tests [3].

Despite the establishment of certification standards, substantial percentages of module populations do fail well before their 25-year warranty. A team associated with the National Institute of Advanced Industrial Science and Technology, (AIST, Japan) recently conducted a performance and reliability audit of 483 residential rooftop installations in Japan commissioned between 1993 and 2006 [5]. They found that up to 16% of installations had experienced partial or whole replacement of the modules. The study cites a dominant failure pathway for Conventional Modules in Japan manufactured in the 1990's and early 2000's: (1) cell interconnects become more resistive, apparently due either to corrosion or fatigue of the interconnect ribbons or solder connections; (2) interconnects resistively heat, which increases the severity of temperature cycling and leads to even higher resistive heating (3) interconnect overheat or breakage leads to backsheet blackening, power loss, or other failure events.

Similarly, a study at the National Renewable Energy Lab (NREL) [6] found that the primary underlying causes of module failures in the field were due to cell/interconnect breakage (40.7%), and corrosion (45.3%) (Figure 3) [7].

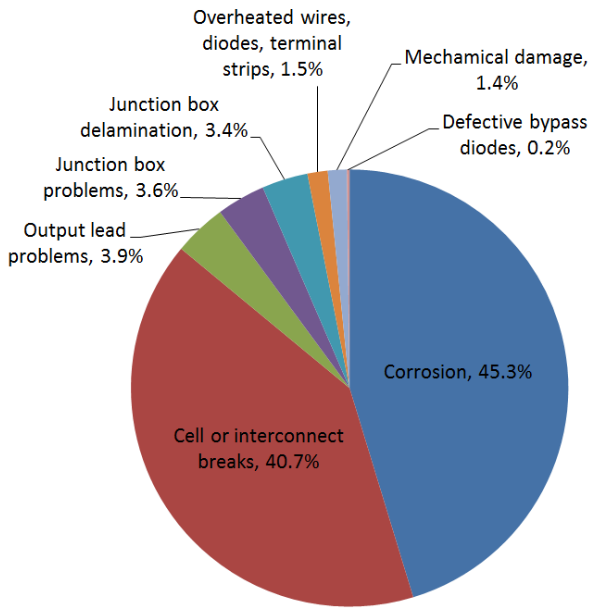

Figure 3: Underlying causes of module failures in the field. SunPower's design mitigates 86% of the typical module failures which affect standard efficiency cells [7]

Real world data is consistent with these studies. SunPower is in the unique position of having purchased two companies which deployed Conventional Modules. PowerLight was a project development company which installed 240 MW of modules from 20 different manufacturers before it was bought by SunPower. This fleet has an average age of 6.7 years, and has a failure rate of 8,700 warrantable returns per million modules installed – nearly 1%. SunPower also purchased a relatively high quality European Conventional Module manufacturer which had installed over 500 MW. This fleet has an average age of 4.6 years and has a failure rate of 1,450 returns per million or 0.14%.

SunPower's current generation module has a rate of only 27 returns per million modules built. This includes all post-site-commissioning world-wide warranty returns of E-Series modules (Jan 2006 through July-2012, 6.5 million modules). With a fleet size of 2 GW, this difference immediately begs the question: from where does this reliability advantage come?

In addition to failure rate, power degradation is a critical module behavior. While outright module failure can abruptly cause downtime and increase operational burdens, a failed module is relatively easy to detect and, once replaced, theoretically restores the site to its expected level of production. However, a power degradation of a few percent has a direct effect on production over a module's lifetime and such a small percent drop would not justify a claim under most module warranties. Further, power degradation typically occurs fairly uniformly across modules of the same design and manufacturing pedigree, so power degradation will generally occur across entire installation.

Various field studies have measured the degradation rate of conventional crystalline modules at between 0.6% per year to 1.5% per year, so a reasonable assessment is 1.0% per year [8], [9], [10], [11], [12] (Figure 4). These studies are discussed further in Appendix A.

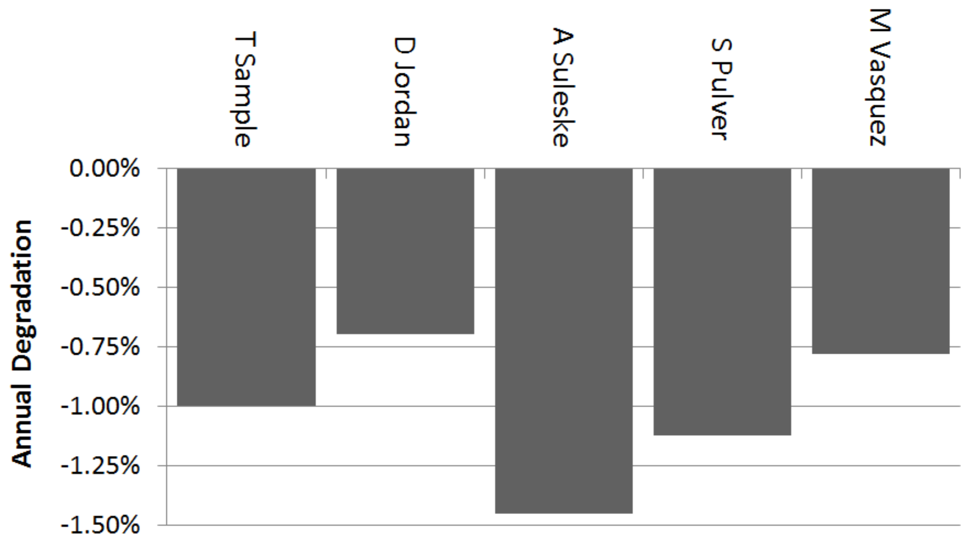

Figure 4: Various studies show annual degradation rates of c-Si modules range from 0.7% per year to nearly 1.5% per year. Module ages range from two to twenty two years.

In order to perform a more robust assessment, SunPower recently completed its own fleet-wide system level degradation study of 445 systems within the SunPower operating fleet. The study included 266 systems (86 MW) using the previous generation of SunPower modules as old as 3.5 years, and 179 systems (42 MW), using Conventional Modules as old as 6 years. Data spanning back to the site commissioning date were used to determine fleet-wide degradation rates, representing 3.2 million module-years of monitored data. The study [13], and a review by independent engineering firm Black and Veatch, are available upon request.

A key result from this study is shown graphically below in Figure 5. The annual system power degradation rate (including inverter) for SunPower systems with the previous generation of modules was found to be -0.32 ±0.32 % (95% confidence) per year, while non-SunPower conventional systems were found to degrade at -1.25 ±0.25% (95% confidence) per year, and in both cases were shown to be linear with time. Experimental and field data are continuing to be collected on SunPower's current generation of module, which will be discussed more in Section III.

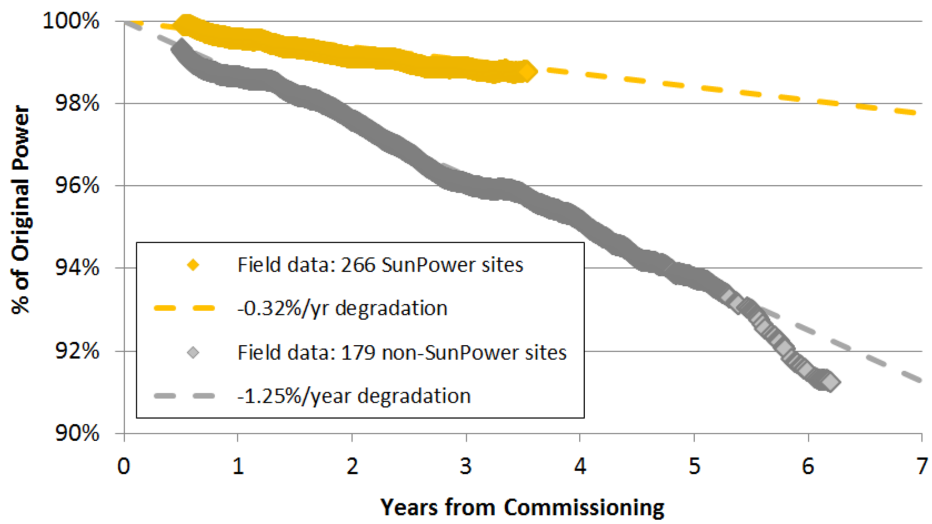

\

Figure 5: Fleet degradation of previous generation SunPower systems (orange) and non-SunPower systems (grey). SunPower systems show an average -0.32% per year degradation rate, compared with -1.25% per year for non-SunPower systems.

Why do SunPower modules have a degradation rate that's so much lower than Conventional Modules? SunPower's back-contact Maxeon cells have important design differences from conventional cells: the key differences in the thick tin-plated high-density copper foundation on the backside of the cell and the use of strain-relieved interconnects offer much higher corrosion resistance and a dramatic reduction of mechanical stress and fatigue at the cell interconnects. This design has been refined through SunPower's stringent internal qualification criteria, which require passing much longer durations than those prescribed for the IEC standard certification test, as well as additional tests not prescribed by IEC.

This section focuses on why SunPower's cell and module design leads to lower degradation rates than Conventional Module designs.

SunPower design differences

Cell architecture and metallization

Conventional cells are made of various grades of monocrystalline or multicrystalline p-type silicon. The front surface is typically textured to enhance light scattering and thus increase absorption lengths within the cell; it is also treated with an anti-reflection coating. The front-surface is also an n-type emitter, typically doped with phosphorus; the back is typically a p-type emitter doped with boron. When the conventional cell is illuminated, electron-hole pairs are formed within the cell, and they are collected at these doped regions and transferred into metal conductors. On the front (sunny/top) side of the cell, metal contacts are typically formed by screen-printing a silver paste into relatively thin and narrow lines in order to maximize the exposed silicon. On the rear, light exposure is not relevant, so the entire surface is coated. A less expensive screen-printed aluminum paste (aluminum mixed with glass frit) is normally used. Once fired, these pastes form a porous and granular structure which does not have strength or ductility.

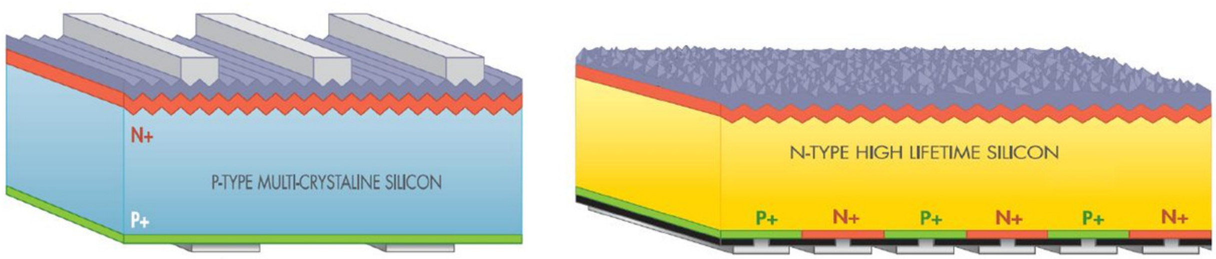

Figure 6: A cross-section representing a conventional cell (left) and a SunPower back-contact cell (right). Images are not to scale.

SunPower's back-contact cells are made of high grade monocrystalline n-type silicon. The front surface is textured and anti-refection coated for maximum light harvesting. Metallization is completely different from the conventional cell. Instead of using granular metal pastes, interdigitated copper fingers are electroplated onto the rear of the silicon, providing strongly adhered solid foundation of ductile metal conductors; these are then electroplated with tin.

Although it is widely understood in the solar industry that SunPower's solid electroplated backside conductors have lower series resistance than metal pastes, it is often overlooked that they also dramatically enhance reliability because they (a) form a stronger bond with the silicon (b) reinforce the cell with solid metal, creating a flexible, crack-resistant, and resilient cell, and (c) have a non-porous structure with tin coating, which is corrosion-resistant.

Cell-to-cell interconnects

To create a module, cells have to be interconnected. From a reliability perspective, these interconnects are crucial, since failure to maintain electrical contact between cells results in total failure of the module to perform, and in the worst-case scenario could potentially result in an arc-fault failure.

Conventional Module manufacturers typically rely on tin-coated copper ribbons, which are soldered along the length of the cell to printed grid lines (Figure 7). Soldering metal and crystalline materials together is considered "state of the art" and still leads to reliability challenges from manufacturing induced micro-cracks and stress from differences in thermal expansion [14]. The cells are connected by "daisy chaining" ribbons that alternate from the front of one cell to the back of the next. As modules heat and cool, the gaps between cells expand and contract, kneading these ribbons back and forth [15]. A recent NREL study [16] has shown that as a result of thermal expansion, they are much more likely to fail within 25 years if not properly strain relieved (in the tabbing ribbon where it traverses between cells, Figure 7).

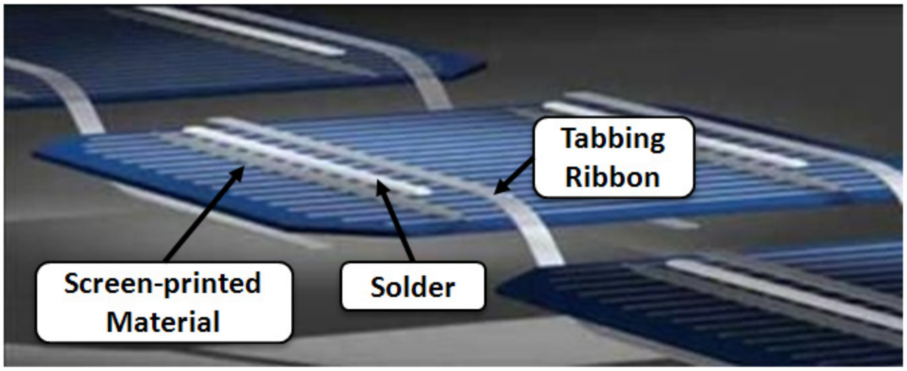

Figure 7: A 3D (exploded) rendering of ribbon interconnections for conventional cells [17]**.**

In contrast, the SunPower cell interconnection is an engineered tab (Figure 8). Instead of bonding ribbons along the entire length of the cell, a stamped metal interconnect is soldered to the edges of the cell. This technique is designed to minimize the effects of thermal stresses in four ways. First, it is attached to the cell using standard solder pads where are part of the copper plated foundation. The soldering of tin-plated copper elements is something that has been widely used in electronics manufacturing for decades due to its proven robustness. Second, they have cut-outs which allow expansion and contraction as the cells grow and shrink with temperature, providing strain relief. Third, there are three solder pads on each side of the interconnect, providing redundancy. In the case a solder joint ever fails, current is rerouted through the remaining pads onto the cell surface, which also has parallel bus-bars to distribute current as necessary. Finally, when there is a "hot cell" due to shading or local soiling, the solder joint does not get as hot because the thick copper interconnect efficiently draws heat away from the hot cell [18], keeping the solder pads cooler. In short, the main failure mechanisms from silicon-metal bonding have been designed out of the cell.

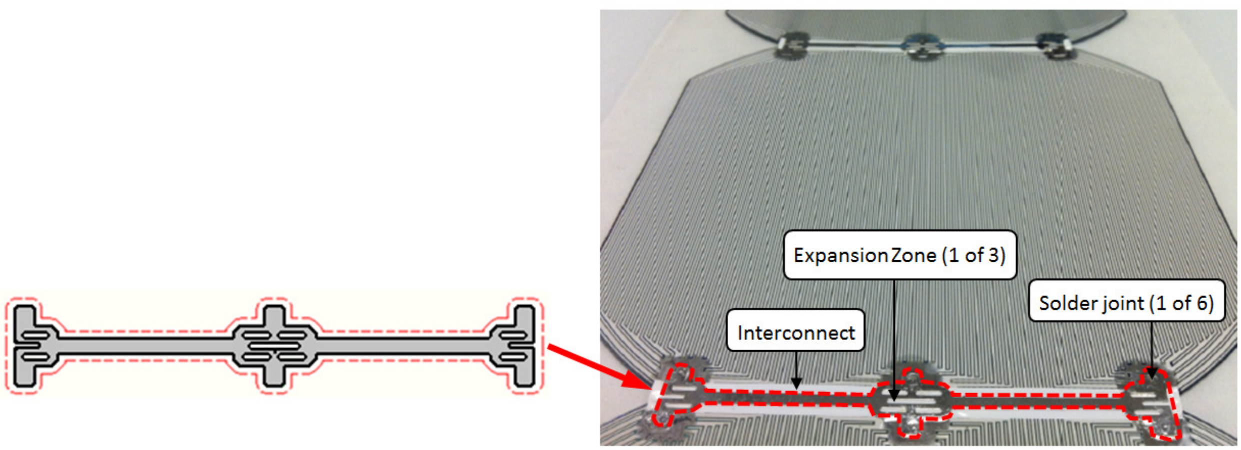

Figure 8: SunPower's cell-to-cell interconnect is designed with strain relief. CAD drawing of the interconnection (left). A string of cells after soldering the interconnect (right). The interconnect is soldered at 3 tabs on the upstream cell and 3 tabs on the downstream cell.

To summarize, SunPower's cell architecture and interconnects are significantly different from Conventional Modules. The differences are visually summarized below in Figure 9.

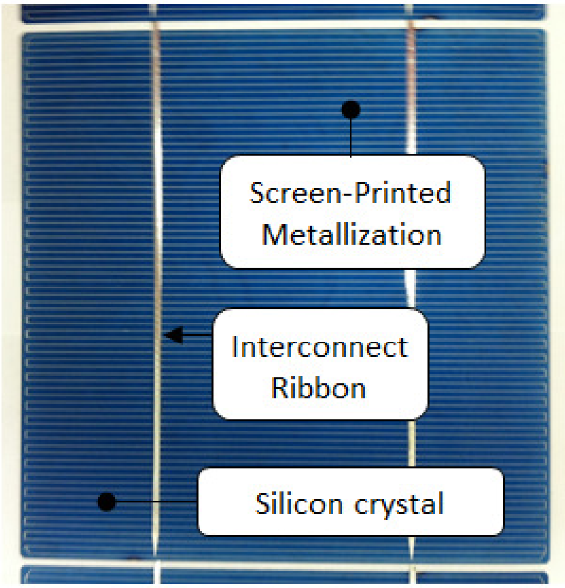

Conventional Cell - Front

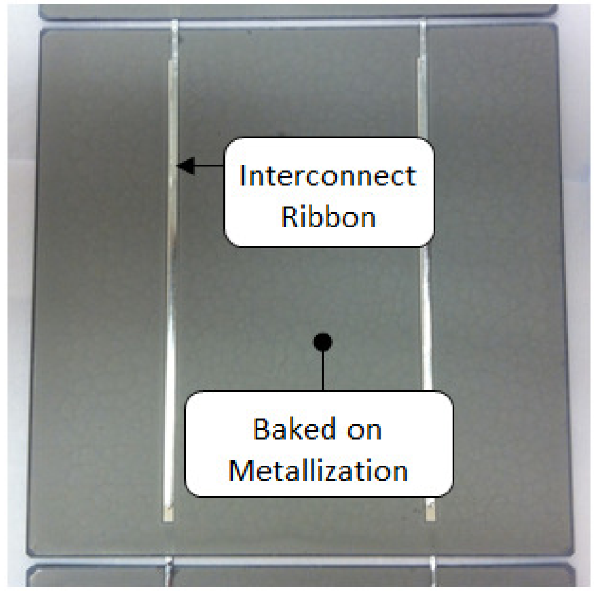

Conventional Cell - Rear

SunPower Maxeon Cell - Front

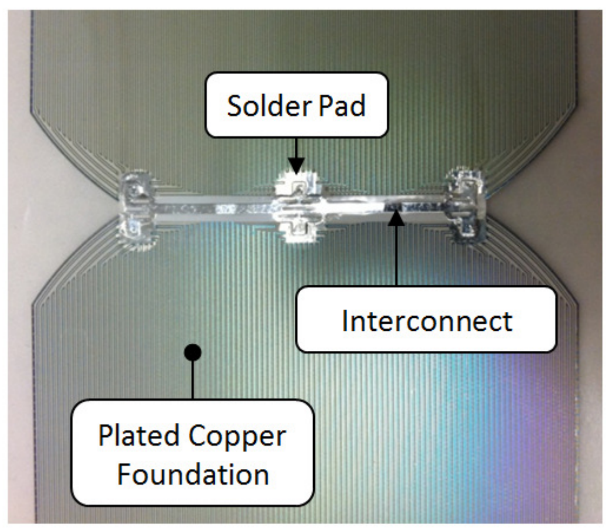

SunPower Maxeon Cell - Rear

Figure 9: Top: typical conventional cells post-stringing. Bottom: SunPower cells post-stringing.

Laminate construction

Figure 10 shows a cross-section of a SunPower module compared with a typical Conventional Module.

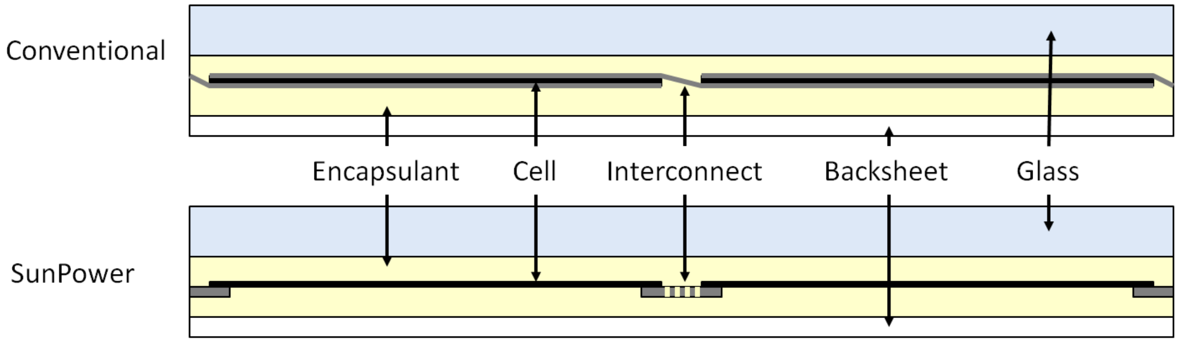

Figure 10: Diagram (not to scale) of a laminate stack cross-section, for a typical Conventional Module (top) and a SunPower module (bottom). Note that a SunPower module also has a thin material above the interconnect which is the same color as the backsheet, so the interconnect does not show on the front of a SunPower module.

The design does not look very different to the casual observer – both have cells encapsulated in a polymer encapsulant that is bonded both to the front side glass and a polymer backsheet. However, the materials and their quality can vary widely and their specific properties can have important impacts on performance.

Materials and suppliers for other laminate components, such as glass, encapsulant, and backsheet, vary between manufacturers, and their specific properties can have important ramifications for long-term reliability. It is beyond the scope of this white paper to do exhaustive comparisons, but SunPower's materials qualification processes have identified a wide variation in quality for these materials.

Design Iterations

SunPower has produced high efficiency cells for decades. The original cell design was intended for use in concentrating applications; however, in the mid-2000s, non-concentrated flat plate modules came into widespread production. The generations of these SunPower modules can be put into three categories:

- **Previous generation**: 2005-2011. These modules required positive grounding. One version:
  - Gen 2 Maxeon cells. Module efficiencies up to 18%.
- **Current generation**: 2011 onward. No positive grounding required. Two versions:
  - E series: Gen 2 Maxeon cells. Module efficiencies up to 20%.
  - X series: Gen 3 Maxeon cells. Module efficiencies up to 22% and better shade tolerance.

Reliable by Design: Results in side-by-side stress testing

As shown in the previous section, SunPower's patented back-contact design is substantially different from the designs used by Conventional Module manufacturers. In this section we present comparisons stress-by-stress, and show how these design decisions lead to better reliability performance.

Results for Damp Heat stress

Humidity and moisture have a significant impact on metal corrosion and hydrolysis of plastics. As water vapor diffuses through a typical module's backsheet and into the EVA (ethylene vinyl acetate) encapsulant, acetic acid is formed. This has the effect of weakening the bonds of the front-side silver contacts and rear-side aluminum metallization. This, in turn, decreases the ability to carry charge carriers, ultimately reducing module performance. It also can accelerate corrosion of the metal, increasing series resistance and reducing efficiency [19]. Finally, although water does not readily diffuse into silicon, it can create local interstitial defects and change the surface recombination rate.

The industry-standard (and IEC 61215 certification standard) test for moisture and humidity effects is the Damp Heat 1000 (DH1000) test, which places the product in an environmental chamber at 85ºC and 85% relative humidity (RH) for 1000 hours. At the time of its introduction as a certification test under IEC 61215 (Ed. 1) in 1993, DH1000 was understood to roughly represent 20 years' exposure in Miami, FL [1]. However, Kempe more recently suggested [20] that 2000-3000 hours may be more appropriate for hot/humid climates such as Miami, FL or Bangkok, Thailand.

(Figure 11, left) shows a side-by-side comparison of electroluminescence (EL) images of a conventional multicrystalline silicon module after DH1000 (IEC certification level) and DH3000 (Kempe's expectation for 20 years in a humid environment). The Conventional Module shows a 28% power loss. This degradation is evidence of water vapor diffusion through the backsheet and around the edges of the cells. This weakens the bonds and corrodes the silver grid lines, resulting in a substantial loss in the ability to carry current. In contrast, the SunPower module (Figure 11, right) appears virtually unchanged. The current carrying copper layer is much more substantial than required to carry the current, proving a large design safety factor. Also it is coated with tin plating, providing a high level of corrosion resistance. The reader will note that the image at far right is not after DH3000, but after DH7750, where it experienced a power loss of 2.7%.

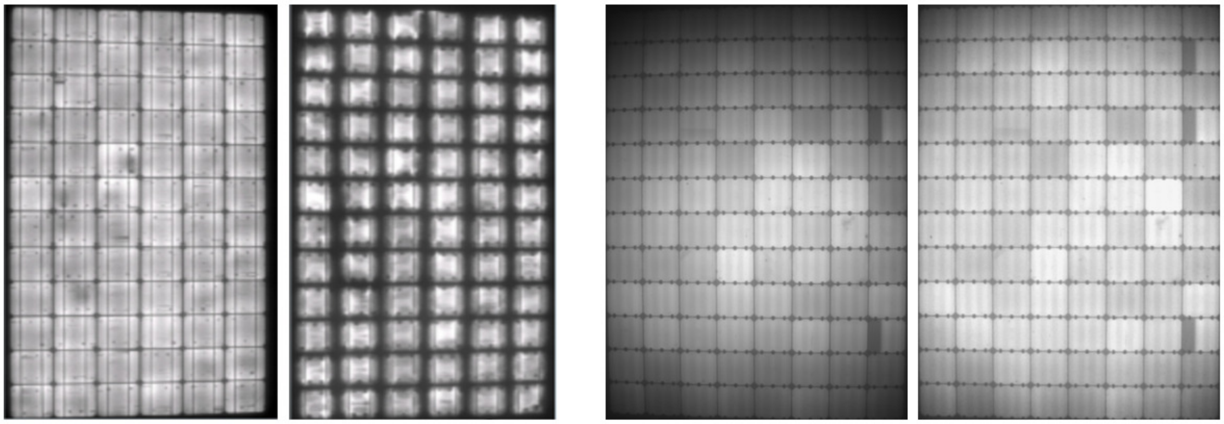

Figure 11: Electroluminescent images after exposure to damp heat for 1000 hours (standard efficiency multicrystalline, left) [21]**. The new black areas show cells/regions of power loss. In contrast, the SunPower cell shows virtually no change after 7750 hours of damp**

Figure 11 gives a more quantitative assessment. The plot shows data a Fraunhofer Institute study [22] for a group of modules from seven (unnamed) Conventional Module manufacturers with at least 100 MW of production per year in 2010. The plot shows performance after increasing hours of exposure to damp heat – well beyond basic industry certifications. Although well-built Conventional Modules fare well up to DH2000, shortly thereafter their power output (normalized by initial output) degrades significantly.

For comparison, SunPower performed testing in the same standard DH conditions (note SunPower's Reliability lab is certified by UL to carry out its own testing to UL standards). Results from two SunPower modules are shown; the first (gray) line is SunPower's previous generation of modules. These show less than 5% degradation after DH3000, while most Conventional Modules show more than 10% degradation and two show more than 50% degradation. The black line shows SunPower's current generation of modules, with less than 3% degradation after DH7500. SunPower's linear degradation indicates that the stress causes steady wear-out, as opposed to abrupt catastrophic failure. This is just one benefit from a series of reliability improvements integrated into the current generation; these improvements will be explained in more detail in Section III of this document.

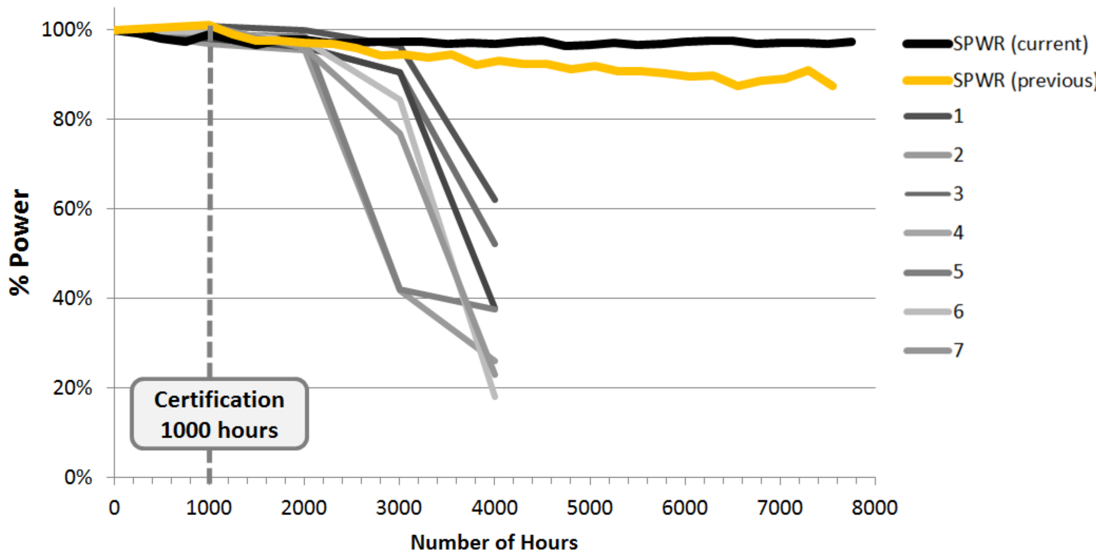

Figure 12: Damp heat testing of seven Conventional Modules and SunPower's previous and current modules. The Conventional Modules show a sharp power drop starting after 2000 hours, while SunPower products remain relatively unaffected beyond 7000 hours.

Dynamic Loading - Effects of wind and snow

Wind, snow, and the weight of an installer who steps on his modules are real-world stresses that modules should be considered. The primary concern in any of these scenarios is that the module flexes, allowing the brittle silicon wafers to crack, which can impact power production in three ways. First, if the crack breaks electrical connections within the cell, then the disconnected portion cannot pass charge carriers out of the cell, causing a "dead zone". Second, a crack can reduce shunt resistance, a measure of the resistance between the front and the back of a cell. Low shunt resistance provides an alternate current path for the carriers, reducing the amount flowing to the emitters and out of the cell. Thirdly, cracks create traps and defects throughout the thickness of the cell, increasing recombination rates and lowering efficiency.

How a cell fractures and what it takes to fracture a cell depend on how the cell is built. In conventional cells, the silicon crystal itself provides the mechanical strength of the cell. The metallization paste is comprised of metallic powders carried in volatile solvents. Wafer firing burns off the solvents, leaving a porous metallic layer which exists for electrical purposes and is not intended to provide structural support. In contrast, SunPower Maxeon cells have thick ductile copper metallization on the back of each cell that provides both high electrical and thermal conductivity, and structural support. The rear of the silicon crystal is plated with solid copper, rather than the porous metal paste applied by conventional manufacturers. SunPower's electroplating process yields consistent, strong, and low stress bonding.

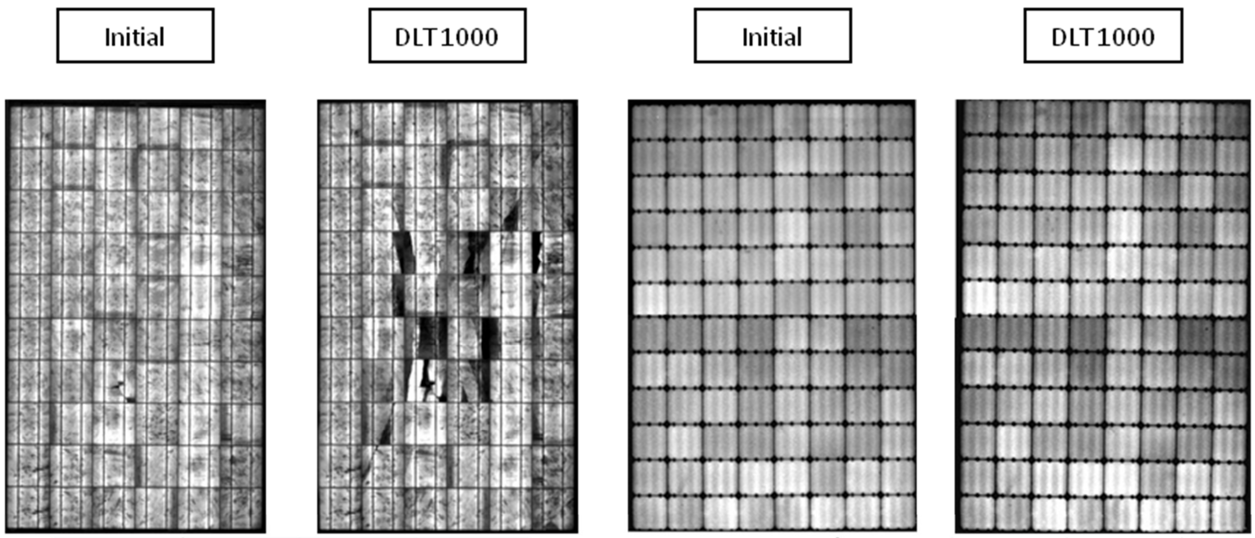

	Initial	500	1000
Power (W)	233.2	232.2	224.2
Power (%)	100.0%	99.6%	96.1%
Rsh (Ω)	2116.1	1694.8	1587.0

	Initial	500	1000
Power (W)	319.1	318.8	319.2
Power (%)	100.0%	99.9%	100.0%
Rsh	7441.1	7411.7	7483.6

Figure 13: Electroluminescent images flash test data after 1000 cycles of dynamic loading to 2400Pa (equivalent to 130mph (209kph) wind), conducted at SunPower. The Conventional Module (left) suffered from power loss while the SunPower module (right) was not significantly affected.

Part of SunPower's design qualification includes a dynamic load test (DLT). In this test, a force of 2400Pa is repeatedly applied to the front and back of the module, deflecting it back and forth. This is equivalent to 50 lb/ft^2 (244 kg/m^2) load or a sustained wind speed of 90mph (145kph) – equivalent to a category one hurricane. This test is designed to ensure that a product can withstand a lifetime of shipping, installation, and environmental stresses and that there are no unfavorable characteristics inherent in the design.

A side-by-side comparison of a conventional multicrystalline silicon module and a SunPower module in this dynamic load test is shown in Figure 13. After 1000 cycles, the standard efficiency module shows several broken cells in the center, and a power loss of nearly 4%. The shunt resistance of this module has dropped by more than 20%, which results in parasitic yield losses at lower irradiance levels [23]. Low shunt resistance can also push cells into reverse bias which leads to more frequent diode activation and yield loss. If the shunt resistance is low enough, or if the diode fails, the cell may form a catastrophic hotspot [24]. The SunPower module, on the other hand, shows no broken cells and no power loss; the shunt resistance appears to have risen slightly but this is within the tolerance of flash testing accuracy.

It is true that 2400Pa of stress corresponds to extreme winds (130 mph, 209 kph) or snow loads (about 3m deep, assuming 80 kg/m^3 snow density) that are unlikely to be observed in real life at most, but not all, installations. Nonetheless a basic tenet of design qualification testing is that larger “safety factors” are generally better, since real-world stresses can come from unexpected events. For example, stresses occur during shipping and installation. An installer weighing 80 kg (175 lbs) stepping on a module with a boot that has a contact area of roughly 3” x 10” (0.019 m^2) induces local normal stress on the surface of the glass of about 41,000 Pa. Fortunately, the glass spreads this stress over a larger area (it bows relatively smoothly), reducing the strain on the cells; but, it is not as forgiving as a uniform pressure applied over the entire surface.

Results for Thermal Cycling stress

SunPower’s engineered interconnect design, electroplated cells, and higher efficiency lead to better performance under thermal cycling stress. Thermal cycling occurs at least one time per day in the life of a module. In cloudy areas where irradiance can vary dramatically throughout the day, a module can experience tens of thousands of thermal cycles throughout its lifetime.

Thermal cycling primarily affects areas where there are mismatches in the Coefficient of Thermal Expansion (CTE). As materials grow and shrink by different amounts, areas where they are bonded to each other become stressed. Since there is a four-fold difference between the CTE of a silicon cell and the metal ribbon used conventional cells [14], the ribbon bond must be carefully designed and manufactured to ensure a reliable module. Some examples of solder bond failure for Conventional Modules are shown in Figure 13.

Figure 14: (left) Hotspots on a fielded Conventional Module caused by manufacturing defects [5]. (right) Dark areas indicate ribbon detachment on a Conventional Module after TC400 [21]**.**

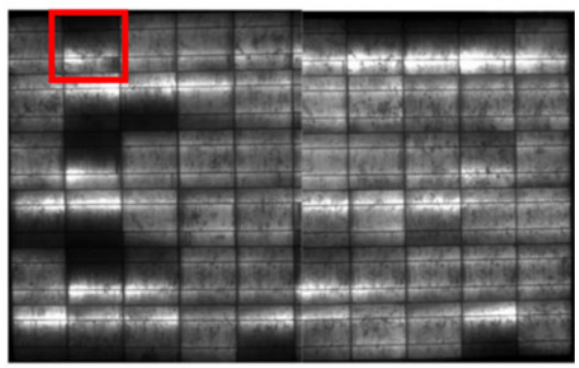

Figure 14: (left) Hotspots on a fielded Conventional Module caused by manufacturing defects [5]. (right) Dark areas indicate ribbon detachment on a Conventional Module after TC400 [21]**.**

The ribbon on conventional cells is soldered along the cell length (Figure 7). Soldering along a long length creates opportunity for stress to be “manufactured in” to the cell, as the ribbon must be connected to the cell at elevated temperatures. When the cell cools back to ambient temperatures, the CTE mismatch between the materials imparts built-in stress to the ribbon-cell interface (Figure 15). This process must be performed within tight parameters, as bonding can cause thermally induced micro cracks to form under the ribbon. Further, the bond between the ribbon and printed grid line is susceptible to thermal stresses in the laboratory and field, which can result in dead zones [14] (Figure 14, right).

Joining metal and crystalline materials in this way is a relatively new technology, the other use being cutting edge MEMS devices [25]. Despite this, a large and diversified group of cell manufacturers and cell types has evolved in recent years. Subtle variations between cells, such as cell thickness, can have very large impacts to mechanical stability and reliability [26]. As a result, manufacturers who use different cell suppliers must constantly adapt their manufacturing parameters to ensure this sensitive process is performed correctly.

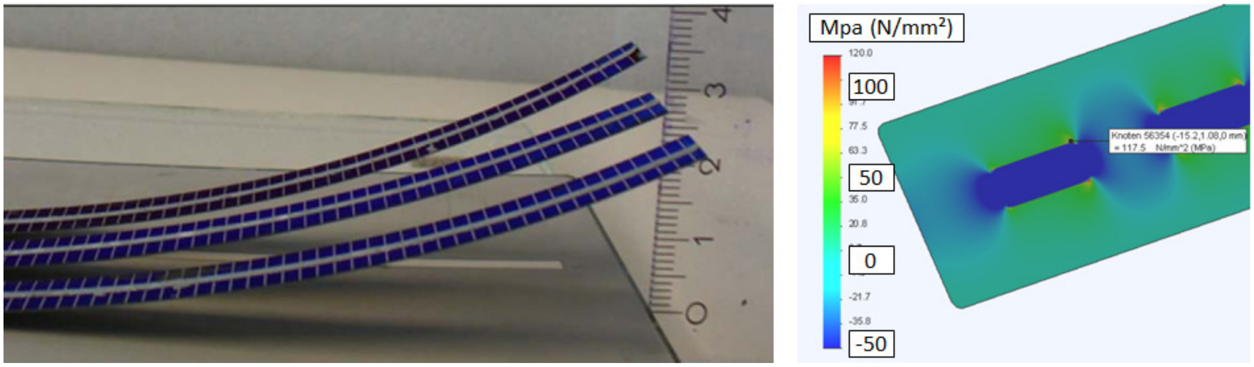

Figure 15: Ribbons contract after solder bake operation. The contraction top of silicon bends cells due to CTE mismatch (left). Finite element analysis indicates built-in stress can be over 100MPa after cooling (right). Blue rectangles indicate locations of solder bonds [27].

In addition to the cell-to-ribbon bond, the treatment of the ribbon *between* cells is another manufacturing characteristic critical to the reliability of Conventional Modules. A recent study by Bosco [16] at NREL concluded that the lifetime of solder ribbons on conventional cells is significantly dependent on thermal cycling, and highly dependent on the details of strain relief. Figure 16 shows two cases: a solder joint with no strain relief and another with an unsoldered length at the end of the cell and additional ribbon which allows for some strain relief. The strain-relieved situation, which may be difficult to ensure during manufacturing, has an approximately 2.5x longer life.

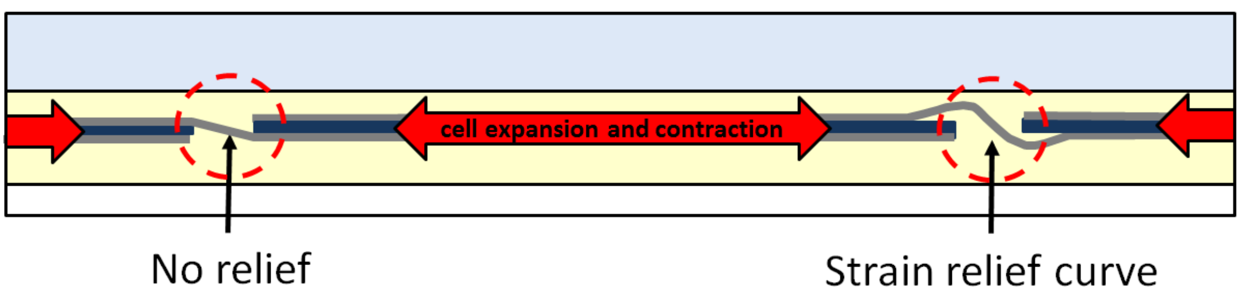

Figure 16: Shows cross section of module (inset from Figure 10). Stringing process on left leaves no strain relief while process on right leaves a strain relief curve. This small detail has a significant impact on reliability under thermal cycling.

In contrast to the ribbon-bond design, SunPower uses a fundamentally different cell connection system: a stamped plated copper interconnect with three cell connections per side and integrated strain relief between cells (see Figure 8). Multiple solder junctions provide redundancy if there is ever an issue with a solder joint, while the strain relief provides robust resistance to thermal cycling. Additionally, long solder joints are avoided through the use of simple solder pads on cell edges, similar to the solder pads used in the integrated circuit industry for decades.

Relative resistance of designs against thermal cycling stress is generally tested through the IEC Thermal Cycling test, which subjects modules to periodic cycles from -40℃ to 85℃. The current IEC standard for the certification of solar modules requires only 200 cycles (TC200). However, the acceleration factor for thermal cycling notoriously is difficult to correlate directly to years of performance. For instance, Wohlgemuth reported [28] that early studies showed “modules that survived 50 thermal cycles [the current standard at the time] began failing after 3-5 years due to broken interconnects and/or broken cells that resulted in total loss of module power.” The acceleration factor for thermal cycling is even less clear in partly-cloudy locations, where there can be several strong irradiance fluctuations per day. Cell and interconnect breaks are dominated by temperature cycling or high-temperature soak failure modes [4].

Figure X shows EL images of Conventional Modules after 200 thermal cycles (left) and SunPower modules after 2500 thermal cycles. After TC200, the Conventional Module degraded by 6.2% due to printed finger detachment in the dark zones. The SunPower module degraded less than a tenth of a percent at TC200 and at TC2500, SunPower degraded less than 2%.

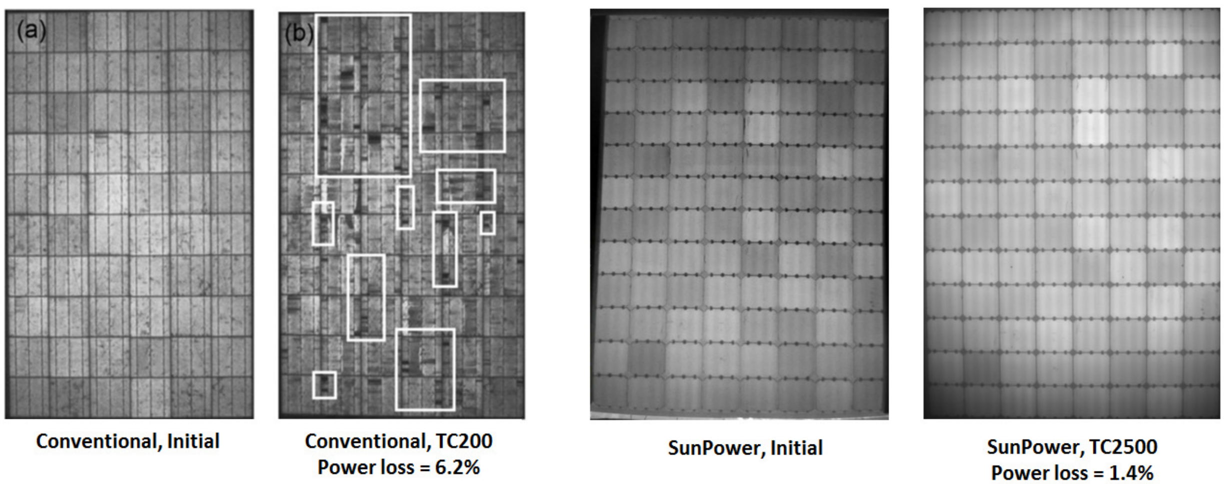

Figure 17: Conventional and SunPower modules in thermal cycling. The Conventional Module degrades over 6% after 200 cycles [29]**, while the SunPower module degradates less than 2% after 2100 cycles.**

SunPower conducted another comparison using internal test data and data for several major unnamed conventional manufacturers who produced more than 100 MW per year in 2010, performed by TÜV and Fraunhöfer Institute, and published by Koehl [22] (Figure 18). The results for the conventional manufacturers vary substantially, indicative of the sensitivity of manufacturing process parameters. Many manufacturers perform quite well for the period of testing; only degrading a few percent even at TC800. However, one product is down 10% by TC400, and down >25% by TC500; two other products are down 8%-9% by TC800. Note that all of these products pass the standard IEC certification standard of TC200. In contrast, SunPower’s current and previous technologies fare exceptionally well in the test, exhibiting only 2% degradation at TC2000, ten times the duration of the IEC certification standard.

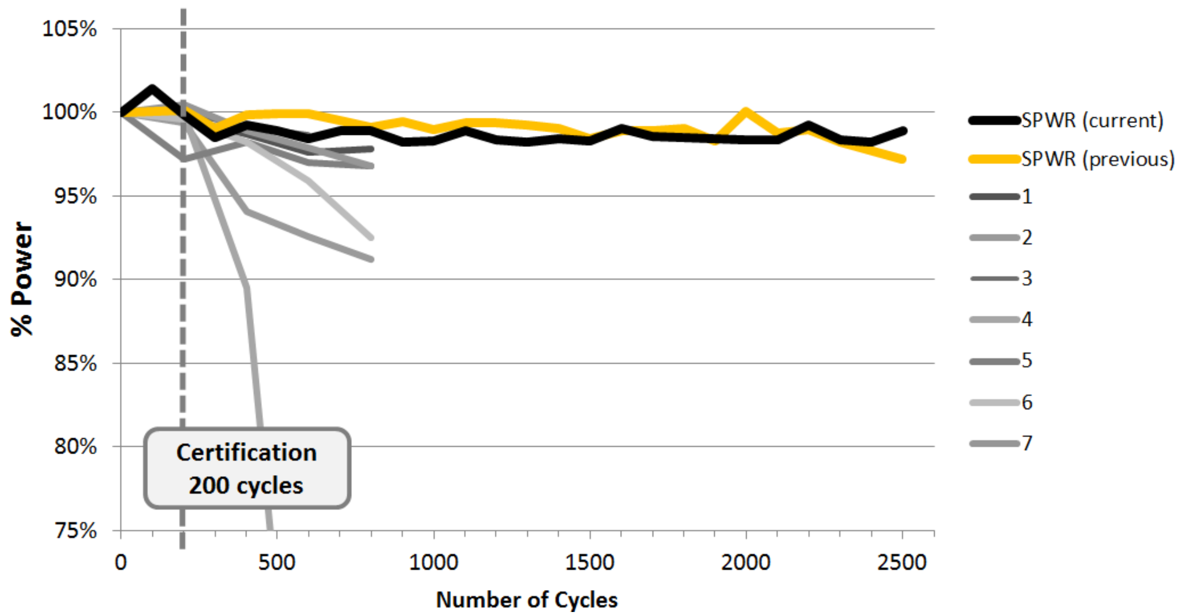

Figure 18: Thermal cycle testing of seven Conventional Modules and SunPower's previous and current modules. The Conventional Modules start to degrade steadily after 200 cycles, while SunPower products remain practically unaffected beyond 2000 cycles.

Results for Partial Shading and Reverse Bias Stress

Solar cells in a module are essentially current sources connected in series. When their current flow isn't perfectly matched, mismatch losses occur and the "weakest" cells can operate in reverse bias. When a cell is in reverse bias it essentially consumes power from neighboring cells and converts it into heat, as opposed to absorbing light and converting it to electricity.

This causes wasted power and potentially damaging heat dissipation in the affected cell. The most common cause of mismatch and reverse bias is due to partial shading, which can occur in a wide range of applications. In residential rooftop applications, common sources are chimneys, dormers, other rooftop protrusions, trees, or utility poles. Leaves commonly fall onto roofs from nearby trees and wet weather promotes their adhesion. Birds may leave droppings across an array, which can also create enough shading to cause reverse bias. In agricultural areas, airborne dust settles on modules and sticks due to the morning dew; if the dew and dust preferentially collects at one end or corner of the module, the partial shading can also cause reverse bias. Finally, cell manufacturing defects can also push cells into permanent reverse bias.

Cell design heavily influences how cells react under these conditions. Once again, SunPower's back-contact design performs differently than a conventional cell, due to fundamental design differences. In the conventional cell, heavily doped layers (regions rich with charge carriers) are separated by bulk silicon, which is lightly doped, creating space between heavily p-doped and n-doped areas on the front and back (see Figure 6, left). When the cell is in reverse bias, the separation between the heavily doped areas creates a high reverse bias voltage.

SunPower's back contact design has steep doping profiles on the backside of the cell, which can be seen where the p-doped and n-doped areas are immediately adjacent (Figure 6, right). These regions are rich in charge carriers, so when a cell is in reverse bias, current flows more easily, resulting in a lower reverse-bias voltage.

As a result, a typical conventional cell has a breakdown voltage of approximately -15V to -20V [30], whereas the SunPower cell's breakdown voltage is only about -5.5V for its second generation Maxeon cells (E-Series modules) and -2.5V for its third generation Maxeon cells (X-Series modules). With a lower reverse bias voltage there is less power, and therefore less heat, to dissipate. Table 1 shows a side-by-side comparison of the heat dissipation between the two designs.

Table 1: Illustrative comparison of estimated cell power dissipation in reverse bias

	SunPower X21	SunPower E20	Conventional Module
Module Power	345	327	240
Number of cells	96	96	60
I_{mp} (STC, amps)	6.02	5.98	8.14
V_{mp} (STC, volts)	57.3	54.7	29.5
V_{Rb} (reverse bias, volts)	2.5	5.5	17[1]
Heat (W)[2]	**15**	**33**	**138**
% Module power remaining:			
with diode	**96%**	**90%**	**67%[3]**
without diode	**96%**	**90%**	**42%**

[1] V_{RB} value from literature [8].
[2] $Power_{Rb} = V_{Rb} \times I_{mp}$, all of this power is dissipated as heat.
[3] % Power = Dissipated Watts / Module Power. Assumes diode shorts 1/3 of the Conventional Module when present. If diode does not activate, assumes power dissipates as heat. Estimate for comparison purposes only.

The power dissipation is not the most pertinent issue; rather, the maximum heat density that can occur, since high heat is what damages the cell, module encapsulant, and backsheet. On conventional cells the breakdown, and subsequent heating, occurs non-uniformly at the weakest points of the cells. These points occur in areas with uneven doping, crystalline defects, trace processing contaminants, etch sites, or edge effects [31]. The heat dissipated through these points can reach temperatures high enough to destroy the module [32] , necessitating the use of bypass diodes as a means of protection. In contrast, the SunPower Maxeon cell has a stable reverse-biased breakdown that happens uniformly across the back of the cell, so the additional energy is dissipated evenly across the full area of the cell and temperatures remain relatively low. As a result, SunPower does not require bypass diodes for reliability.

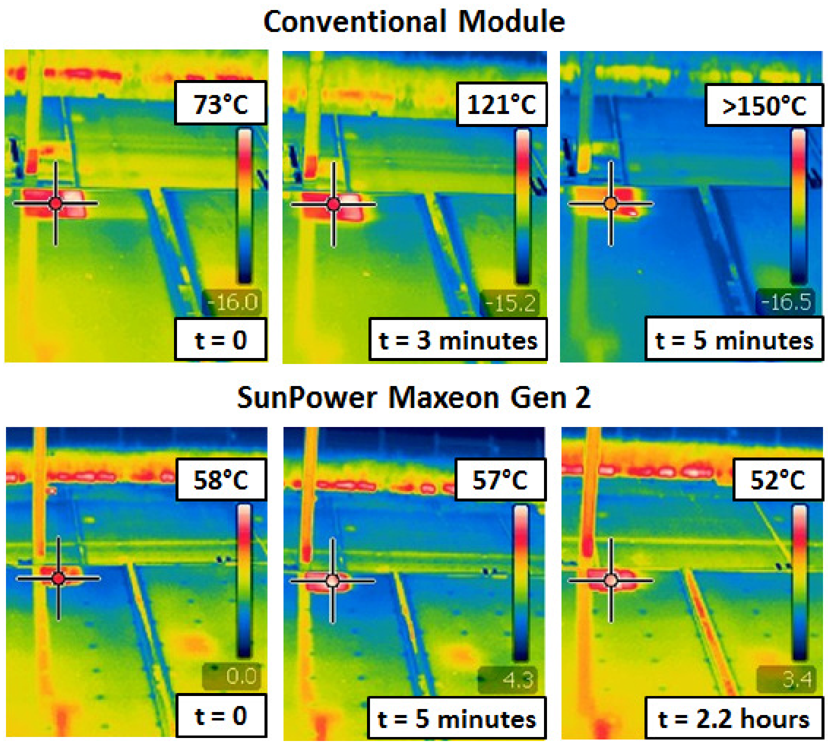

Figure 19: IR images of arrays of Conventional (left) and SunPower (right) modules at approximately 840 W/m² and 24°C ambient temperature with shade over a cell and diodes removed. The Conventional Cell exhibits an edge hotspot of more than 150°C within five minutes, while the SunPower cell exhibits relatively uniform heating, even after more than two hours. This occurs due to SunPower's low reverse bias voltage.

Manufacturers generally install diodes across substrings within the module (Figure 20). These substrings almost always divide the module into thirds (20 cells in a 60-cell Conventional Module or 24 cells in a 72-cell Conventional Module). When a conventional cell is shaded, the voltage drop across the cell is limited to the voltage produced by the other cells within its sub-string, and a large fraction of the current is shunted through the bypass diode, deactivating the substring.

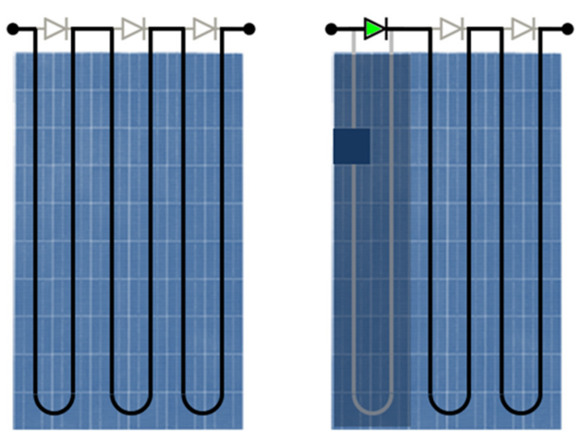

Figure 20: Substrings within a Conventional Module operating normally (left) and with an activated bypass diode (right). The module with the activated bypass produces two thirds of the power of the module without diode activation.

It might seem counterintuitive that a higher reverse bias voltage is generally a desired trait for Conventional Module manufacturers, since it raises the temperature of a cell in reverse bias. However, a higher reverse bias voltage ensures a bypass diode will activate at lower threshold, making the module more sensitive to reverse bias conditions, such as partial shading or cell defects. While this module design initially protects against thermal breakdown, there are two potential side effects – production and long term reliability.

A lower threshold for bypass diode activation means partial shading or soiling are more likely to activate the diode. When the bypass diode activates, the voltage contribution from that substring is eliminated, reducing power proportionally. In a typical Conventional Module, a single cell perpetually in reverse bias will effectively reduce a 240W module into a 160W module.

Further, an activated diode runs at an elevated temperature reducing the remaining life of the diode. All diodes will eventually fail; and, the life depends on temperature as well as several other factors, including module design, diode quality, junction box heat transfer, and module installation. Depending on how a diode fails, it can either permanently remove a substring from that module's production or allow a shaded cell to run in reverse bias unmitigated, causing high heating in areas of a conventional cell which allow current to flow, generally causing backsheet damage.

SunPower cells operate in reverse bias with uniform breakdown across the cell, resulting in much lower temperatures, so bypass diodes are not required to ensure long term reliability. SunPower does include diodes in its J-boxes, but the diodes do *not* turn on when only one cell is shaded. The voltage drop across a single reverse-biased cell is not sufficient to drive significant current through the diode. SunPower includes diodes only to increase the production of the system in the case that several cells in the same substring go into reverse bias. In this case, the diodes limit the total amount of power that can be dissipated by reverse-biased cells.

Light-induced degradation

Light-induced degradation (LID) is a very fast degradation mechanism which drives an efficiency loss of 1-4% in p-type silicon within hours of exposure [33], [34], [35]. It was first discovered in 1972 by R. L. Crabb [36], and since then, the mechanisms have been comprehensively studied, culminating with a model and strong evidence for boron-oxygen complex formation by Schmidt [34] and Glunz [37]. The fact that it occurs only in p-type, and specifically boron-doped silicon (e.g. gallium-doped Si does not exhibit LID) leads to an obvious advantage for Maxeon cells, which are n-doped both on the front surface and in the bulk. This mechanism has been covered in numerous journal articles and trade publications.

Summary: Design Differences

SunPower modules have several intrinsic differences over Conventional Modules which result in superior resistance against real world stresses. The use of n-type silicon prevents early degradation due to LID. The thickly plated, tin coated copper foundation of the Maxeon cell is highly resistant against the forces of moisture and oxidation. This metal foundation allows for thinner, more flexible silicon, resulting in a cell which can withstand repeated snow and wind loading and can crack without significant power loss. Electroplating the metal directly onto the cell ensures a strong and uniform bond with low residual stresses. Solder pads and an interconnect that allows for thermal expansion are used to connect the cells instead of a process intensive copper ribbon solder bond. This gives the cell extreme robustness against thermal cycling. Finally, the low breakdown voltage permits more cells to be shaded before diode activation and each cell has built-in diode protection so the reverse-bias breakdown is not damaging and is uniform across the cell, which prevents thermal runaway, regardless of diode health. SunPower's X series modules, which make up an increasing portion of the product mix, has even better reverse bias characteristics, resulting in an even more shade tolerant module.

Table 2: A summary of cell design differences and impacts on reliability

Component	Conventional Design	Maxeon Design	Reliability Benefits
Bulk Silicon	Mono or multi crystalline, p-type, boron-doped	Monocrystalline, n-type, phosphorous-doped	n-type Si has no boron in bulk so no LID. (boron is on rear emitter, where no UV is present)
n-emitter	Entire front surface, phosphorous-doped	Backside, phosphorous-doped; interdigitated via lithography	Lack of front side emitters reduces impact of certain degradation modes (see Section II). Also allows for better front-surface passivation since the front surface need not also serve as electrical contact.
p-emitter	Entire back surface, boron-doped	Backside, boron-doped; interdigitated via lithography	
Front metal contact	Baked silver paste, resulting in porous frit	None	SunPower cell maintains structural integrity even if cracked; conventional cell falls apart when cracked, relying on encapsulant for support. Conventional has porous metal, which has high surface area and relies on encapsulant and backsheet to have a low
Back metal contact	Baked aluminum paste, resulting in porous frit	Electroplated copper and tin	
Cell interconnection	Tinned copper ribbons; strain relief not intrinsic to design, may be created during stringing process. Solder along length of cell.	Tinned stamped-copper engineered interconnect with built-in strain relief	Conventional ribbon stringing and lamination must be carefully controlled to ensure strain relief between cells; SunPower ensures it by design. SunPower also eliminates a common conventional cell degradation mode excess flux from soldering which can result in front side delamination and reduced output.
Reverse Bias	High breakdown voltage. Current flows in concentrated areas. Relies on bypass diode to protect module.	Low breakdown voltage. Current flows uniformly across cell. Diodes used for performance only.	SunPower design removes a single point of failure, since cells are passively safe from high temperature reverse bias even in the event of a failed bypass diode.

Part II: Reliability Research and Performance Degradation Model (PVLife)

Introduction

SunPower has developed a physical model based on extensive research that addresses SunPower's degradation mechanisms. However, models quantifing Conventional Module degradation is not included, since data and research is, for obvious reasons, primarily focused on the SunPower design. The ability to quantify degradation rate has been vital to SunPower in order to securely offer its current industry-leading twenty five year warranty. Degradation rates cannot be determined through industry standard certification tests such as thermal cycling, damp heat, humidity-freeze, and mechanical load. These tests have been identified as important in assessing reliability [38]; however, they are not designed to estimate useful lifetime because they do not show a strong correlation with field performance and degradation. Instead, these tests are designed to ensure safety and identify infant mortality issues due to basic manufacturing quality [28] [21].

Therefore, SunPower engages in basic fundamental research, supported by both accelerated testing and field data. Research on all key degradation modes are integrated into a cell-by-cell, hour-by-hour performance model that has been validated and published in scientific conference proceedings [39], [40], [41]. Understanding the fundamental physics of failure leads to rapid identification and optimization of design and manufacturing process variables which affect degradation and failure. This section will present key findings from research on the primary degradation modes for SunPower modules:

- Cell damage induced by ultraviolet (UV) radiation
- Photo-thermal encapsulant browning
- Polarization and high-voltage degradation, a.k.a. potential-induced degradation (PID)

This section will also address two key failure modes that likely govern the life of modules:

- Backsheet cracking due to relative humidity (RH) and hydrolysis
- Solder-joint failure due to temperature cycling

Additional degradation and failure modes are also modeled; but, are not discussed because they do not have a significant impact on the degradation or failure rate. These include:

- Soiling
- Reverse-bias cell degradation
- Humidity degradation
- Cell cracks
- Metal corrosion
- Ion migration.
- Encapsulation adhesion failure
- Diode failure.

Bypass diode failure from temperature soaking has been studied, but is not considered a key failure mode due to the passive reverse bias protection in SunPower cells (see Table 1).

All of the degradation modes are integrated into SunPower's proprietary performance degradation model, known as "PVLife", which is described here in detail. As a result of this model, SunPower is able to estimate its "degradation budget", that is, how much degradation is due to various degradation modes. As shown below in Figure 21, SunPower's previous generation of modules degraded primarily due to encapsulant browning, then polarization, and then cell UV degradation. Its current generation has made tremendous advances by essentially eliminating polarization and substantially reducing encapsulant browning, but allowing for slightly more cell UV degradation. SunPower's reliability research and resulting PVLife model allows us to rationally design modules to optimize performance while still improving reliability by quantifying these tradeoffs.

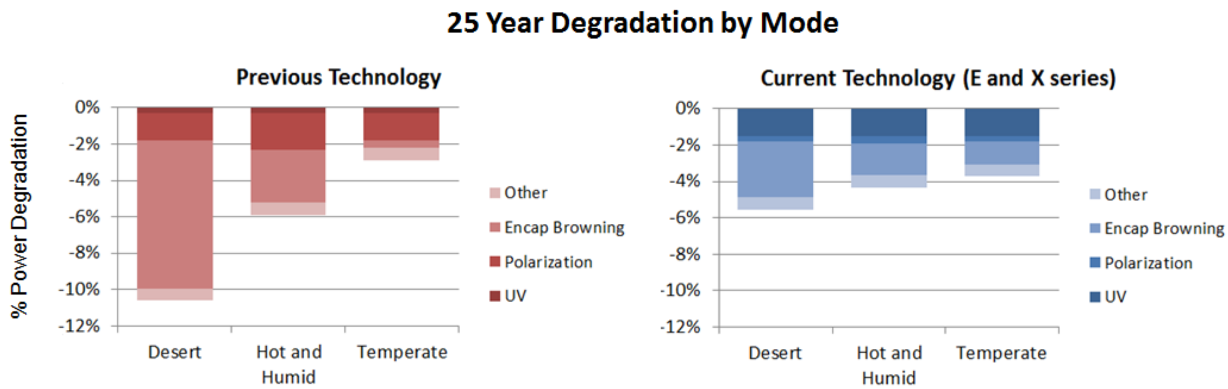

Figure 21: Module degradation budget for previous and current generation in typical environments generated by PVLife.

PVLife Physical Model Framework

PVLife is primarily a physical model, not a statistical or "reliability block-diagram" model. The intent is to solve for a specific system/array's degradation rate, given the module used, its electrical and physical configuration, its mounting, and the weather and irradiance expected. PVLife solves the coupled electro-thermal equations that predict module performance for a given set of weather conditions in order to obtain cell temperature and electrical condition; at each hour of the (simulated) day for every day of the system's life. It independently computes the incident spectrum, electrical operating point, and temperature of each individual cell. PVLife uses this electrical and thermal solution as input to physical sub-models for the key degradation and failure modes and computes incremental degradation and chance for failure during each time-step in the simulation. Also, different modes are coupled via the electro-thermal solver. For example the model captures a scenario such as a "weak" cell (due to a certain degradation mode or non-uniform soiling) that gets warmer than its neighbors due to mismatch, which then causes accelerated encapsulant yellowing, which exacerbates the mismatch and causes a run-away situation because of the interdependence of those failure modes.

PVLife predictions compare well with laboratory accelerated testing data as well as field data obtained from various SunPower product monitoring efforts. These results serve to validate the electro-thermal model, degradation sub-models, and increase the understanding of the coupled effects of degradation. In this way, PVLife is a useful tool in SunPower's Design for Reliability program.

The analyzed field data of the previous generation of SunPower modules compares very well with the PVLife simulations as shown in Figure 22.

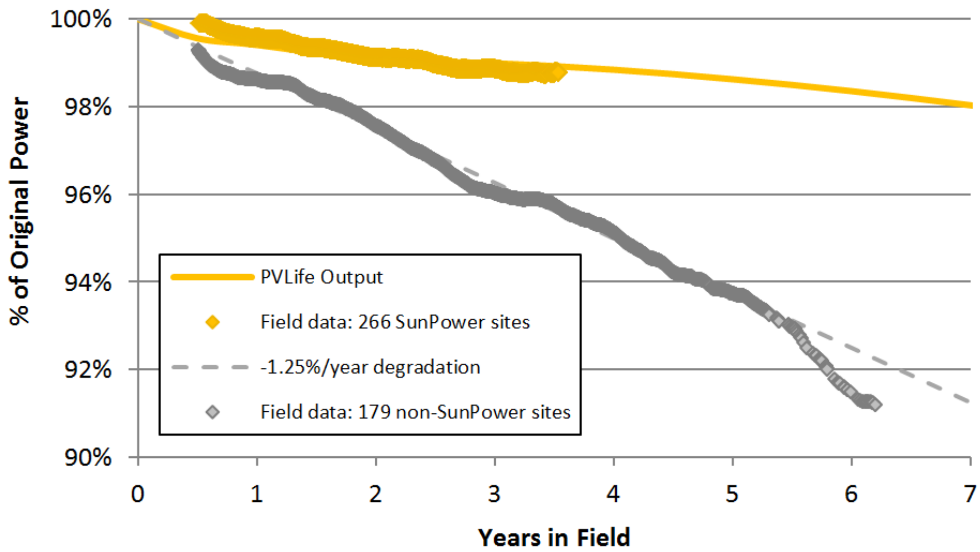

Figure 22: Comparison of PVLife and analyzed field data from the previous generation of SunPower modules.

Electrical and Thermal Model

The one-diode approach to the system modeling used by PVLife is documented thoroughly in PV textbooks. A single solar cell is modeled using the equivalent circuit below (Figure 23). It consists of a photo-generated current source in parallel with a diode and a shunt resistor, all in series with another resistor. Parameters are obtained by fitting actual cell and module performance data to this reduced model.

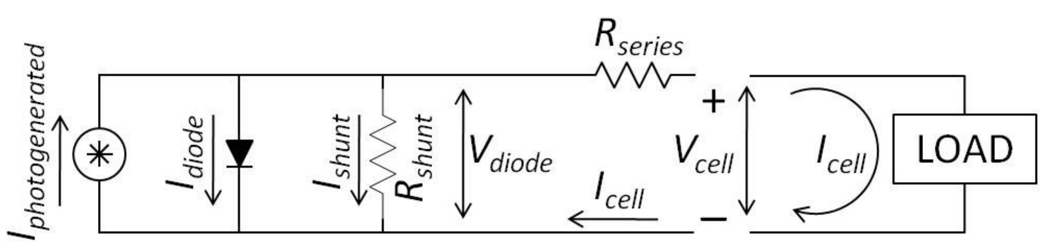

Figure 23: A one-diode model of a solar cell.

A module substring is modeled by solving for all of the one-diode parameters and voltages of all of the cells in the substring and the current through the substring, subject to the constraints of Kirchoff's Laws. A module is modeled by combining substrings and bypass diodes to solve for the system. PV systems are modeled in the same way. The solution at a given time-step in the life of the system yields the voltage, current, and temperature for every cell and diode. Module J-box bypass diodes are modeled by the Shockley equation and the expression for avalanche breakdown current in reverse bias, and are incorporated into the module circuit using Kirchoff's Laws.

Radiation and convection from the module surface above and behind the cell can be grouped together in a Newton cooling law expression and the delta between ambient temperature and the module surface temperature. Measurements were used to determine the value of the loss coefficient empirically. An expression for the temperature difference between a cell and the module surface, based on the module type, rack mounting and irradiance is provided by the PV Array Performance Model from Sandia National Laboratories [42]. Temperature of the bypass diode is calculated using the assumption that the thermal resistance is lowest from the bypass diode to the front surface of the module, and so other heat pathways could be neglected. Therefore the bypass diode temperature depends on the power being dissipated, the measured thermal resistance, and the module temperature directly over the junction box housing the diodes. Coupling of the module temperature with the bypass diodes and junction box is neglected, even though they are known to affect module temperature because of the slightly greater thermal resistance where the J-box is attached.

Irradiance, Glass, Encapsulant and c-Si Response

The solar spectrum is calculated using the SPECTRL2 C-code provided by NREL [43]. When available, data for turbidity, aerosol optical depth, atmospheric water vapor, ozone and albedo are used, otherwise the NASA 1976 atmosphere [44] is used. Functions for transmission, absorption and reflection are used to determine how much irradiance is incident on the cell. If bare cell measurements are used then the measured or predicted external quantum efficiency (EQE) of the glass/encapsulant/cell stack is used, otherwise, the AOI and air mass (AM) functions from the Sandia model [42] are used.

Integration of Degradation and Failure Sub-Models

The flowchart in Figure 24 outlines PVLife's overall algorithm. Because degradation rates are many orders of magnitude slower than the rate at which each cell reaches electrical and thermal equilibrium, there is no attempt to solve coupled electro-thermal and degradation equations. For each hour the degradation leading up that hour is incorporated into each cell's performance; however, for the duration of that hour the electrothermal behavior is assumed to be constant (which neglects a miniscule amount of degradation does occur during that hour). This de-coupling simplification has a negligible impact on accuracy and greatly speeds solution time.

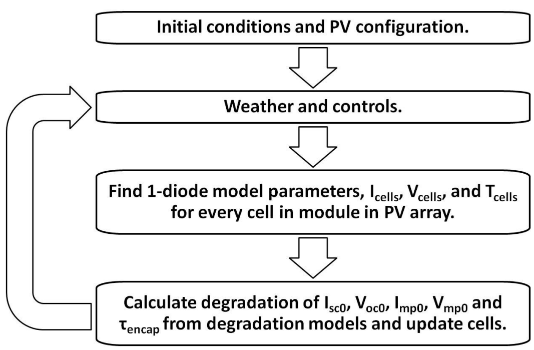

Figure 24: Flow chart of PVLife model.

Inverter and Max-Power-Point-Tracking (MPPT)

The inverter is modeled using an inverter model originated at Sandia National Labs [45]. In general maximum power point tracking (MPPT) is done using a bounded golden section search method, which is robust for global minimization problems with local minima.

SunPower has conducted studies on the electrical performance of central inverters over time to measure degradation over time. Results indicate that there is no measurable power degradation due to the inverter. Instead, inverters effectively function at their rated efficiency or shut down. So while inverters may affect plant availability (uptime), they have not been shown to have a significant effect on system degradation [46].

Degradation Mode: UV-Induced Cell Degradation

All solar cells are, by design, exposed to insolation constantly. As photons are absorbed into the cells, they are converted to current carriers (electrons and holes). Ideally, all of these carriers leave the cell as electricity; however, they may recombine within the cell, resulting in less power output. Less recombination results in a more electricity leaving the cell and a more efficient solar cell.

High energy photons in the UV spectrum can cause damage to the front surface of a cell on the atomic level. A photon can knock an electron out of place in the front surface, creating a small defect. These defects can act as recombination traps which reduce the efficiency of the cell. The kinetics of this type of damage is referred to as the UV damage rate.

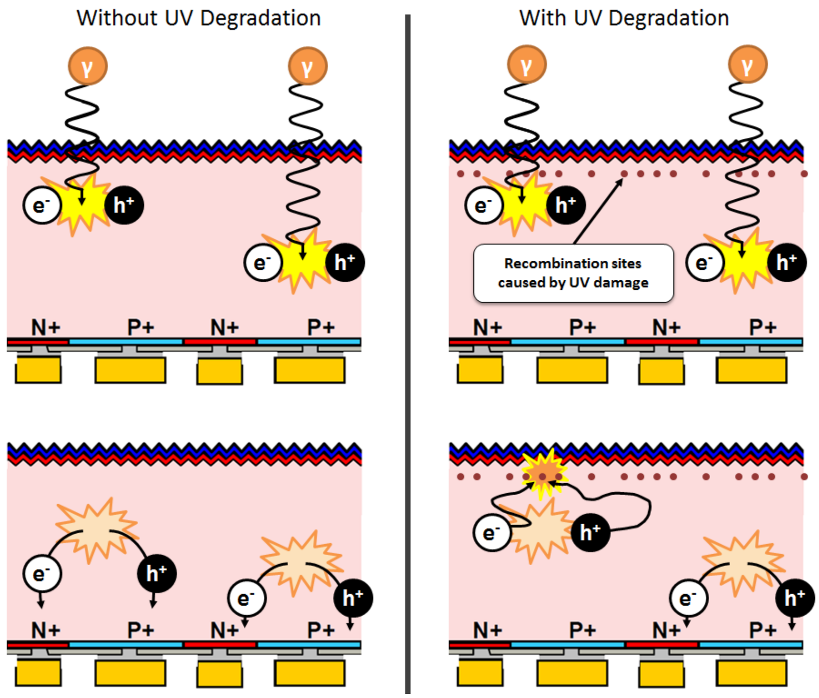

Figure 25: Electron-hole splitting caused by high energy photons in an unexposed cell (left) and UV damaged cell (right). When UV damage is present, charge carriers (especially those created near the front surface) recombine at traps near the front surface, releasing heat instead of producing electricity.

Opposing this UV damage rate is an annealing reaction that is temperature-driven. As the cell is heated, the crystal structure around dislocations "heals" itself, reducing recombination traps. The kinetics of this recovery is referred to as annealing rate. Both phenomena occur simultaneously and balance out at some equilibrium point. For SunPower cells, the UV damage and annealing rates come to equilibrium approximately two weeks after initial field installation, followed by a very slow secondary degradation rate.

To determine the UV damage rate, samples were placed under different bands of UV light and the damage rate was measured. The change in J_0, the surface recombination rate, was found to be a strong function of wavelength and exposure. The resulting function aligns well with measured data (Figure 26). Further details are available in previous publications [40].

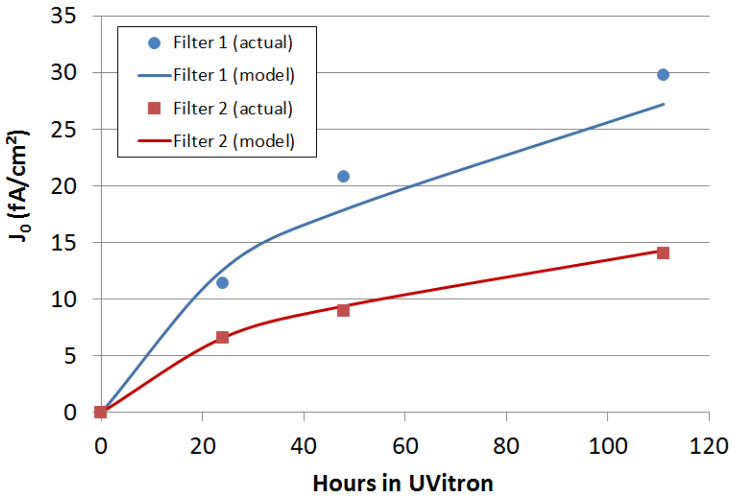

Figure 26: The measured and modeled J_0 increase versus time for test wafers under two different filters. As seen from the graph below, the modeled degradation predicts the measured degradation well.

To determine the annealing rate, damaged test structures were placed in an oven at different temperatures and the recovery was measured over time (Figure 27). The annealing rate is modeled as an exponential decay.

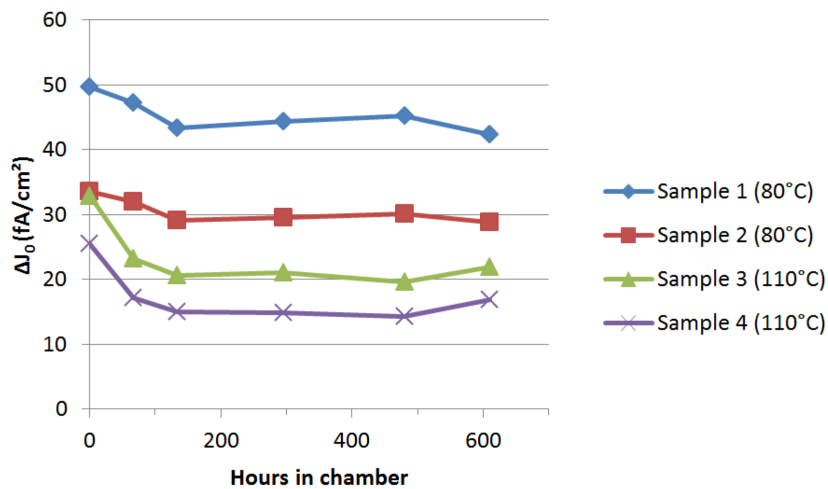

Figure 27: Cells with different levels of damage were recovered at 80°C and 110°C and the annealing rate was observed. Higher J_0 (y-axis) indicates more damage. Recovery is characterized by a fast initial rate followed by a slow rate. Experiments conducted at temperatures as low as 50°C exhibited similar behavior.

The equilibrium point was found by exposing samples to different intensity UV sources. Change was found to follow a power relationship to exposure, with lower equilibrium points corresponding to lower intensity UV sources (Figure 28).

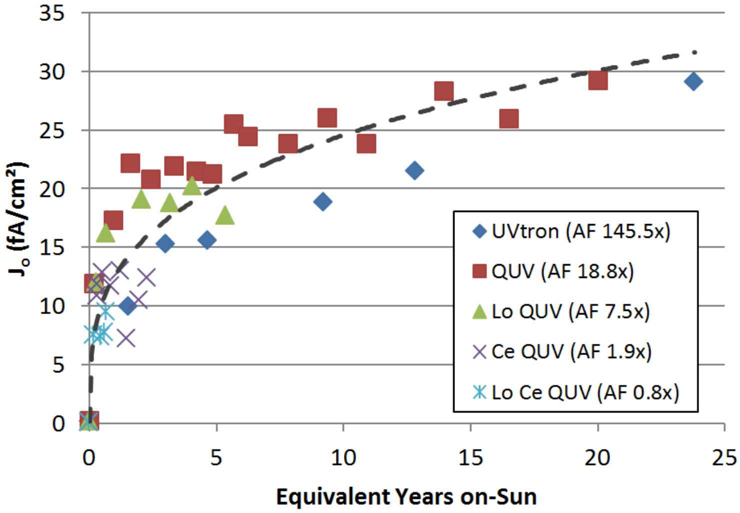

Figure 28: Measured Average J_0 Change versus Equivalent Years on-Sun across five light sources with different intensities of UV exposure. Equilibrium occurs at lower J_0 with lower intensity UV damage sources. Samples at higher intensities did not reach complete equilibrium because all samples were held at 55°C, so the annealing rate did not increase proportionately with higher UV damage rates.

Once an equilibrium model was established, it was validated against measured values, where there was good agreement (Figure 29, red). J_0 values were used to determine efficiency and electrical parameters of the cell through the use of a proprietary model, derived from the Sinton Cell Model [47]. Finally, this model was used to estimate J_0 in the field (Figure 29, green circle). The model also shows that the equilibrium point is fairly insensitive to the annealing rate, where a ten times slower annealing rate equilibrates to approximately two times more damage.

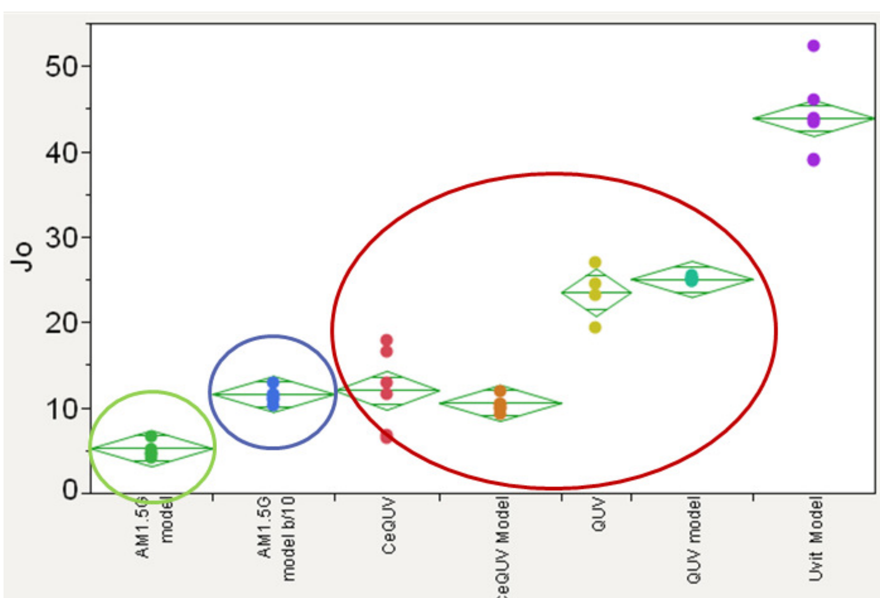

Figure 29: Measured (points) and predicted (diamonds) equilibrium Jo versus light source. There is good agreement between model and measured J_0 from AM1.5G to QUV (~20x intensity). The high intensity (145.5x intensity) UVtron model predicts an equilibrium level; but, none is found in experiments.

From these fundamental experiments and corroborating field exposure tests it was determined that SunPower cells have an initial degradation and secondary degradation rate in 1-sun light. UV degradation reaches a steady equilibrium point on both previous and current generations. The rates of UV degradation and annealing were measured and used as inputs for a UV degradation model. Total degradation from UV is not expected to exceed 2% at twenty five years (Figure 21).

Degradation Mode: Encapsulant UV-Induced Yellowing

Modules use layers of encapsulant to hold the module laminate together, electrically insulate cells, and protect against certain environmental stresses. Encapsulant is found between the glass and cell as well as between the cell and backsheet. As an installed module ages, the color, clarity, or overall transmissive properties of the encapsulant can change, strongly affecting the total amount of light that reaches the cells and, subsequently, the amount of power produced. This is visually evident as “yellowing” of the encapsulant; in extreme cases the encapsulant can turn amber brown as shown in Figure 30 (left). Generally, the yellowing of encapsulants is caused by the photothermal generation of radicals inside the plastic, which react with the molecular backbone of the polymer to create various unsaturated chromophores. As with most photochemical processes, the reaction rate is dependent on the wavelength and intensity of light, as well as the overall system temperature [48], [49]. Figure 30 (right) shows an example of the change in the transmission spectrum that can result. As shown by the different results for normal vs. a “hot” (reverse-biased) cell, encapsulant yellowing is a strong function of temperature.

Many solar encapsulants are designed with UV absorbers (UVAs) which are photoactive chemicals imbedded throughout the film that block the most damaging solar rays from penetrating and interacting with the polymer matrix. Unfortunately, just like any sunscreen, these UVAs have finite lifetimes because they are prone to photothermal oxidative degradation over time. The reduction in protective screening must be taken into account in order to extrapolate degradation rates of EVA over time.

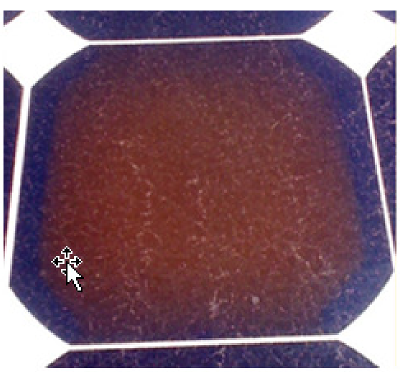

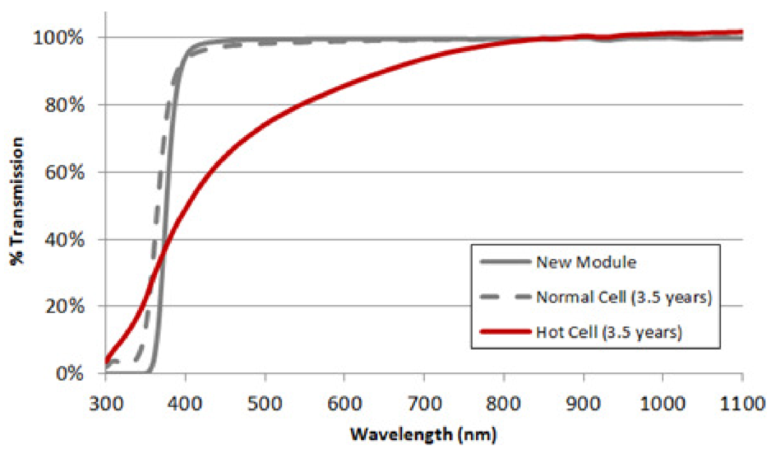

Figure 30: Photothermal browning of encapsulant over a cell that spent about 3.5 years in constant reverse bias during daily operation (left). Transmission spectrum of a sample of encapsulant over a normal cell (dashed grey) and a reverse-biased cell (red) for the same period of time.

Although UVA degradation does not directly cause encapsulant yellowing, the two reactions are optically coupled to each other in space and time because the UVAs filter out the incident light necessary for the yellowing reaction to initiate. Initially the UV light can only penetrate a short distance through the encapsulant and therefore only the top few micrometers can become discolored. However, as the UVAs are progressively destroyed throughout the thickness of the film, damaging UV penetrates further into the film and the overall rate of optical transmission loss increases, as shown in Figure 31. Eventually the system will begin to run out of UVA's entirely; depending on the kinetics (and availability of reactants) of the yellowing reaction, the rate of degradation may reach a maximum at this point, and then eventually slow as reactants are consumed.

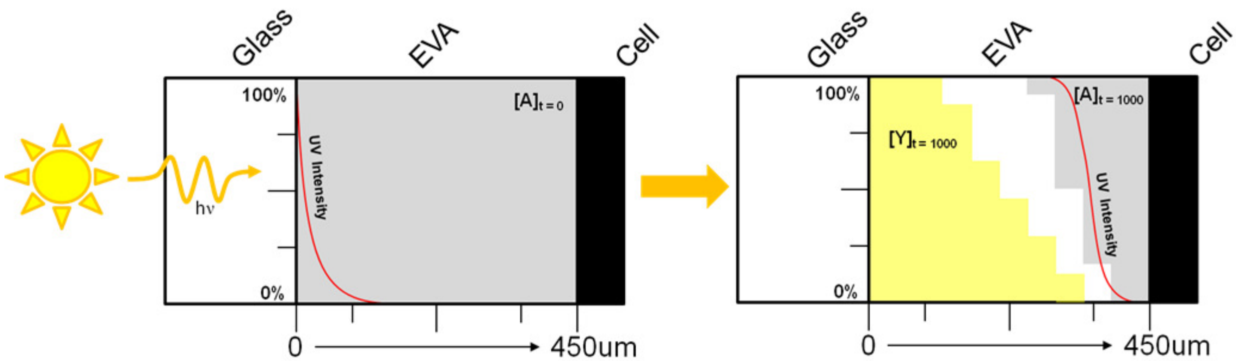

Figure 31: Illustration of UV absorber bleaching followed by the formation of yellow chromophores at time zero (left) and after 1000 units of time (right).

A simple model for this process, published by SunPower [39], is a two-step kinetics mechanism. The first kinetic step is photo-bleaching of UV absorbers, *A*, which is modeled as a 1-step reaction shown in Equation (1), where *B* is the photo-bleached absorber. The second step is a first-order reaction for the conversion of polymer moieties, *R*, to yellow chromophores, *Y*, shown in Equation (2).

$$A + h\nu \xrightarrow{k_1} B \qquad (1)$$

$$R + h\nu \xrightarrow{k_2} Y \qquad (2)$$

These two reactions are coupled by Beer's law for the UV absorption and combined into a pair of partial differential equations that can be solved analytical for steady-exposure and steady-temperature cases [39]. Curve fits of this model vs. accelerated test data were performed in temperature-controlled (50, 80, and 110C) UV exposure of thickness-controlled samples at 20X and 1.4X intensity to ensure linear damage with exposure intensity (i.e. a test that's half the time and double the intensity will have the same result) to obtain activation energies for the reactions as shown in Figure 32. In the PVLife model, a numerical solution is used to handle arbitrary irradiance and temperature when simulating system behavior with real-world weather files.

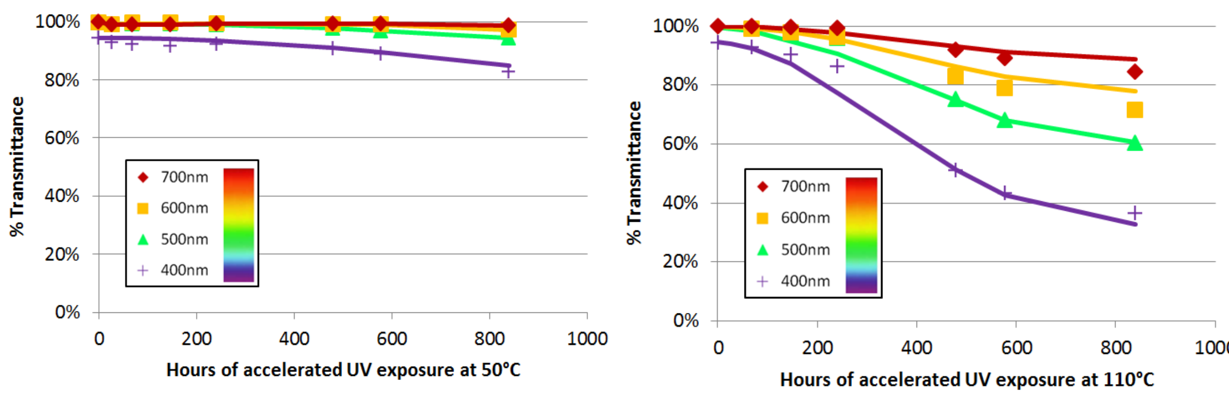

Figure 32: Accelerated laboratory test data for a typical EVA encapsulant, compared to 2-step kinetics model. Optical transmittance degradation is measured at 400nm (blue diamonds), 500nm (green squares), 600nm (yellow triangles) and 700nm (red circles) due to UV exposure at 50C (top plot) and at 110C (bottom plot). Predictions using the simplified 2-step kinetics model for encapsulant browning are shown for the same wavelengths by solid lines of corresponding color. Note the initial period showing no degradation while UV absorbers are being photo-bleached.

One important effect to note is the temperature dependence of the observed transmittance loss. At 50C for example, transmittance loss at λ = 500nm over the 800-hr accelerated experiment was observed to be less than 7%. However at 110C the loss is nearly 40%. This observation qualitatively agrees with that of numerous previous researchers who note that "hot cells" often exhibit browned EVA on the sunny side of the cell [50]. The activation temperature (E_a/R) of the secondary browning reaction is approximately 4700K, meaning that 10C temperature differences can lead to 65% differences in reaction rate. In fact, a 3C difference results in a 15% difference in browning rate. This implies that the 25-year performance of most EVA in the market is likely strongly dependent on temperature. Based on SunPower's 2-step kinetics model and accelerated lab data, in extreme-temperature environments, such as Phoenix Arizona the expected degradation due to this mode is approximately 1.75% over 25 years using SunPower's tracker mounting systems; the rate can be higher on residential rooftops. Note that the model is conservative (in that it over-estimates real-life degradation), since it does not incorporate an oxygen-driven clarifying reaction that is often reported in the literature [51]. That this reaction is present is visually evident from clear areas near the edges of cells, where oxygen has been able to diffuse through the back-sheet and between the cells, into the front-side EVA, as can be seen by the clearer encapsulant around the edges of the hot cells shown in Figure 30.

Degradation Mode: Polarization and High Voltage Degradation

There is some confusion in the industry around voltage stress, and partly due to jargon. SunPower was among the first companies to encounter and report a phenomenon where, on the previous generation modules, efficiency would drop significantly if the negative DC lead was grounded. SunPower's founder, Prof. Dick Swanson of Stanford University, was the first to understand the phenomenon. He called the effect "polarization" [52], and realized that polarization was reversible. SunPower patented a permanent solution [53], simply configuring the modules with the positive lead grounded.

A team within SunPower's R&D division later noticed that, even when the positive lead was grounded, if the modules had high leakage current it was possible to observe yet another degradation mechanism, which SunPower internally called "high voltage degradation" (HVD), since it occurred primarily on cells/modules with very high (negative) bias relative to ground. One of the primary root causes, in both cases, was leakage current from the cell front surface to the (grounded) frame. The differences in the polarity of bias (and current flow) in the two cases leads to different degradation mechanisms.

Conventional Module manufacturers have observed similar phenomena, especially with the advent of transformer-less inverters that allow the string to "float" so that part of the string is biased positive and part is biased negative relative to their grounded frames. Research groups have coined the term "Potential Induced Degradation" (PID), noting that positively and negatively biased modules may have different PID behavior [54]. Conventional Modules typically use p-type Si and have electrodes on the front surface of their modules so the minority charge carriers are electrons. With the electric field pointed toward the front surface of the cell, the potential wall induced by boron doping is lowered so that the concentration of the minority carriers is increased, raising surface recombination and lowering power. SunPower has not adopted this nomenclature yet as it is not yet clear that the detailed mechanisms are the same between SunPower's polarization and HVD mechanisms.

Leakage Current and "Gating"

Both polarization and HVD have a strong dependence on leakage current. In a large string, up to +/- 1000V bias can result in a small leakage current through the front of the cell which reduces power output. However, the electrical configuration depends on the type of frame. Figure 33 (top) shows a cross section view of a solar module with a frame. Any water present on the front surface of the glass has much higher conductivity than the glass, and creates a condition where essentially the front surface of the glass may be treated as being at an isopotential of ground. It is noted, however, that there are really two leakage current paths: glass surface to cell (I_1) and cell to cell (I_2). Leakage current I_1 *only* occurs when the front surface of the module is wet, for example during a rain storm or in early morning dew – when the module surface is dry, ohmic contact between the cells and the frame, via the glass, is quite poor. Assuming uniform resistivity of the encapsulant, I_1 is dependent on the voltage of the cell with respect to ground. I_2 depends on the resistance and voltage between the cell and its nearest neighbors.

Figure 33 (bottom) shows the case for unframed laminates and non-conductive frames such as SunPower's T5. In this case, if the front surface is wet, since the module frame is not necessarily in good contact with ground, the front surface is floating, and thus is near the average voltage of the cells within the module.

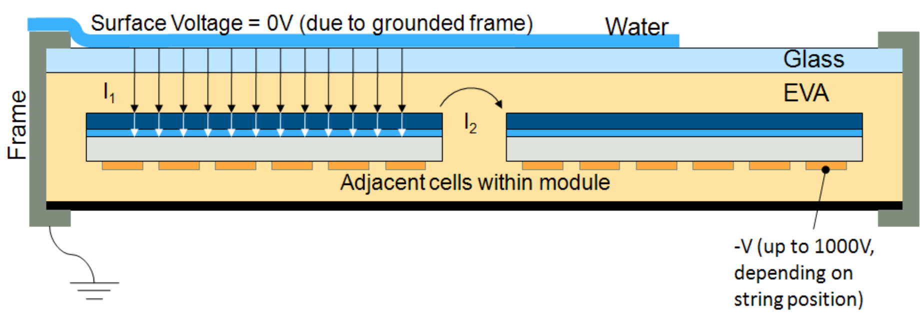

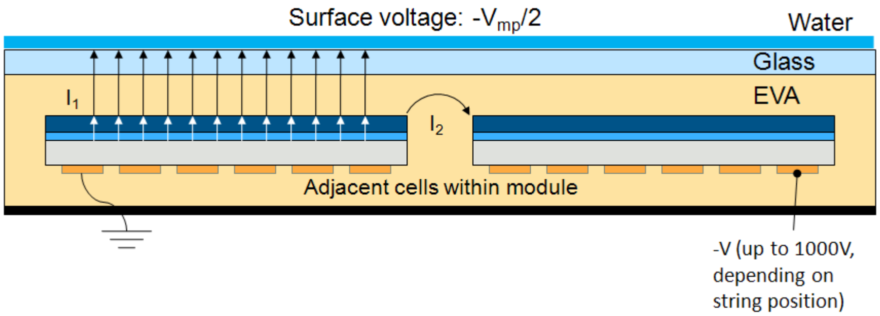

Figure 33: Module cross section shows leakage current paths for modules with grounded metal frames (top) and for modules without frames or with non-conductive frames (bottom).

In order to model the leakage current behavior as a function of glass surface resistance, an outdoor experiment was conducted in which leakage current was measured along with module temperature and dew point. The experiment revealed that module temperatures within 5ºC of the dew point temperature result in a conductive glass front surface. This can occur as the modules start production and bake off morning dew at sunrise, or during rain, but not otherwise.

Polarization – SunPower cells at (+) bias (negative grounded modules)

As shown in Figure 6, SunPower's cells are n-doped on the front surface. The reason for this is to create a diffusion barrier that prevents minority carriers (holes) from diffusing towards the front surface, reducing recombination losses at traps on the front surface. However, if the cells are at a positive potential relative to the front surface of the glass, and leakage current can be conducted through the encapsulant, then a space charge region will form with an accumulation of negative charges at the front surface of the cell. This will partially offset the electric field from the front-surface n-type doping via band bending. Depending on the resistivity of the encapsulant and the amount of resistance at the front surface of the glass due to moisture, polarization can happen relatively quickly but is reversible [52] because when the external potential is withdrawn, the space charge region will gradually discharge as well.

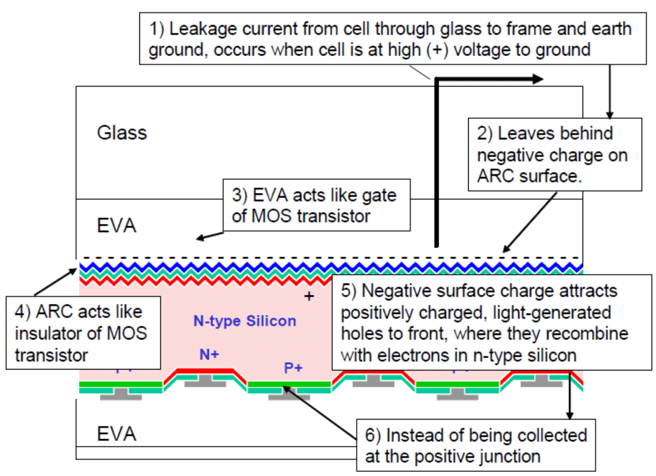

Figure 34: How "polarization" develops on a back contact cell that is positive-biased relative to the glass front surface.

SunPower installations using the previous generation of modules are positively grounded so that the cells are in negative bias, dramatically reducing polarization. However, this is not completely effective due to small leakage currents I_2 between adjacent cells, called "cross-talk polarization". These currents are generally quite small compared to I_1, because the voltage differences between adjacent cells is at the most about 13-14V, compared to up to 1000V in the gated-glass situation. So ironically, polarization was initially discovered as being the most pronounced at hot/humid sites with negative-ground metal-framed modules; but now with positive-ground modules, these sites have the least impact from polarization because gating is frequent and I_1 quickly reverses any cross-talk polarization due to I_2 for all but the cells closest to ground in the string.

PVLife calculates both contributors to polarization using experimental data and the model of Swanson [52]. The magnitude of the effect is about 1% in a hot/dry site, one of the worst scenarios for cross-talk polarization. This is shown in a PVLife simulation in Figure 35, which includes *several* degradation modes on the previous generation – polarization is just responsible for the ~1% annual fluctuation saw-tooth pattern which is superimposed on the mean degradation.

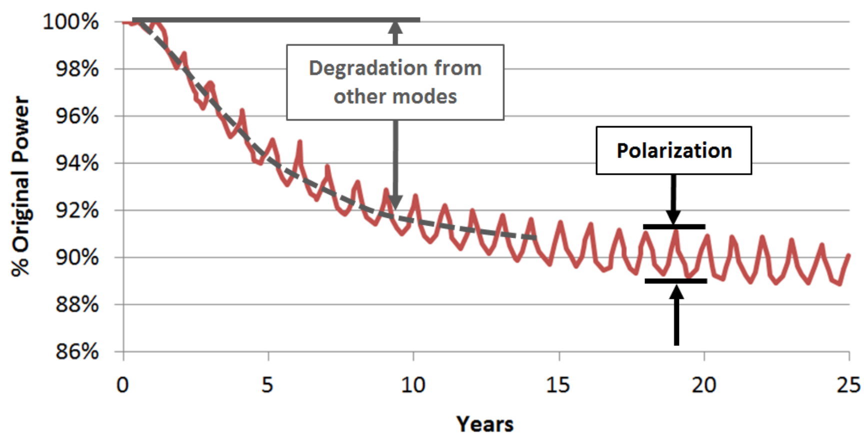

Figure 35: Fluctuations in module performance in a hot/dry environment due to cross-talk polarization on the previous generation. The effect is reversed each year by seasonal rain/gating.

Despite this being a small effect, SunPower has sought to reduce polarization to near zero effect in its current generation of modules, which is so resistant to polarization that it can have any sort of grounding (positive, negative, or ungrounded).

High-Voltage Degradation (HVD) – SunPower Cells at (-) bias (positive-grounded modules)

Although it is a much slower effect than polarization, even in negative bias, there can still be degradation via a different mechanism. In negative bias the development of space charge can create high electric fields near the protective oxide layer. Usually the barrier height at silicon/oxide interface is high enough that no electron can be injected from silicon side, except with the assistance of UV-photon (UV degradation) or hot carriers from avalanche breakdown (reverse bias degradation). However, the thermal oxide layer on the cell is an excellent insulator compared to EVA and glass, so a buildup of space charge region inside the EVA will apply a high electric field across the oxide. A few volts can be generated on an oxide film of thickness on the order of a few tens of nanometers. In this case, the barrier for electrons will be a "triangle" barrier with fixed height and width determined by the local electric field. Fowler-Nordheim (FN) tunneling will then be the dominant conduction mechanism [55]. In crossing the barrier, the electrons are in a high electric field and they will introduce impact ionization and in general an avalanche process. Semi-permanent defects (electron or holes) can be created inside the oxide film. These have been reported in silicon semiconductor manufacturing, especially in the field of flash memory [56], where similar threshold voltage shifts will change MOSFET function [57].

SunPower has developed a model based on this phenomenon to create a model for HVD degradation. While the model is too complicated to describe herein, the model depends on leakage current (whether via I_1 or I_2 paths) and is based on the following:

- During high voltage degradation (HVD), carriers (electrons) are tunneling from silicon side to oxide film. Due to higher local electrical field, the barrier at Si/oxide interface is now a triangle barrier, allowing F/N tunneling. The higher the electrical field, the narrower the tunneling barrier, and the larger the tunneling current.

- After tunneling, electrons will be in the middle of oxide film if oxide film is thick enough or electrical field high enough, or combination of both. They will experience acceleration and collision similar to Zener / Avanlanche break down. Defects are created in the oxide film and they provide trap energy levels for the following electrons. The electrons trapped inside would be permanent charges, unless slowly released by UV exposure.

- There is “fast burn” and “slow burn” related to this process due to a self-blocking effect which has been reported in other semiconductor industries, *e.g.* flash memory. Initially the tunneling will only be fast and is a function of local electrical field. Eventually, the permanent charges accumulated in the oxide film will push up the barrier and cancel out the external electrical field. After that, the degradation will be much slower. The transition point (total interface charge accumulated) would be a function of the external electrical field.

A simple model constructed based on these observations was created and compared to experiments to determine the a few tunable parameters. Lab experiments were conducted where aluminum foil was placed on the surface of the glass of mini-modules, or coupons, in order to simulate a conductive layer of water. Different leakage currents were obtained by adjusting the temperature and the voltage of the cell. Efficiency and voltage change over time was measured to determine the rate of degradation and fit globally over a number of experiments.

It should be noted that the details of real-life temperature and humidity are crucial to understanding the acceleration factors of such experiments. HVD degradation relies on the local electrical field across the oxide, and this does not equal the average electric field in the EVA. When external bias is applied to the glass/EVA/cell sandwich in accelerated tests, the conductivity and susceptibility of these three materials is dramatically different, and space charge will be build up in the first few hours of an accelerated HVD test. After polarization is set up, the local electric field can be 5-10 times higher than the average value and HVD degradation starts. If, however, the bias is halted and the module is held overnight, the polarization will go away and the charge distribution across EVA regains uniformity. The existence of reversible charge accumulation implies that continuous accelerated tests can over-state the risk of HVD degradation. Usually significant leakage current will only occur in the first half an hour of every morning when the module is gated due to dew.

Based on calculations using this model, the effect of HVD on the most-biased modules previous generation modules, biased at -1000V, creates 2% degradation over 25 years in high-humidity environments such as Miami, FL. In hot/dry climates such as Phoenix, AZ, the total degradation expected is negligible over 25 years.

Failure Modes

The previous sections have discussed the primary degradation modes that cause slow degradation in performance. In this section, the failure modes that cause module failure are discussed: backsheet cracking and delamination as well as solder joint failure. Diode failure is also modeled, though it is not a significant failure mode, due to the non-destructive reverse bias characteristics of SunPower cells.

Failure Modes: Backsheet delamination

The backsheet has two primary functions. The first is to provide electrical insulation between the module circuits and the outside world for safe operation of the module. The second is to act as a mechanical and environmental barrier from stresses such as moisture, airborne chemicals, diffuse UV light, and dust. Tertiary functions include cosmetics or secondary power enhancements. Backsheet failures can lead to increased degradation, low system performance, and even an unsafe operating condition.

Backsheet materials primarily degrade from exposure to high humidity and high temperature environments [58]. In these conditions, the bonds are weakened by hydrolysis, which lowers mechanical strength and ductility. When the strength or ductility drops below the operational stress in backsheet material, it can crack and/or delaminate [59], [60], [61]. The operational stress in the backsheet originates extrinsically from the physical loading of the modules from wind or snow; also, it intrinsically originates from the expansion mismatch between the materials in the PV modules. As a result, when interface adhesion strengths drop below the stresses present in the laminates, layer delamination occurs. Photographs of backsheet bubbling in the field (likely caused by an outgassing event elsewhere within the module) and a badly detached and cracked backsheet found on fielded Conventional Modules can be seen in Figure 36.

Figure 36: Backsheet bubbling and separation on Conventional Modules found in the field. Modules were fielded for less than ten years.

The most common method to test backsheet materials against this aging mode is the damp heat test in which modules are exposed to elevated humidity and temperature (85% RH and 85°C) for an extended period of time. The acceleration factor for this test is highly material dependent. Samples were exposed to DH and then standard tensile strength and interface adhesion strength were measured. SunPower's backsheet materials exceed the most commonly accepted criteria of no failure after 1000 hours of DH85/85. In addition to not failing, the experiment above shows that the backsheet materials used in SunPower PV modules still maintain most (>70%) of their initial strengths even after 2000 hours of DH85/85 (Figure 37).

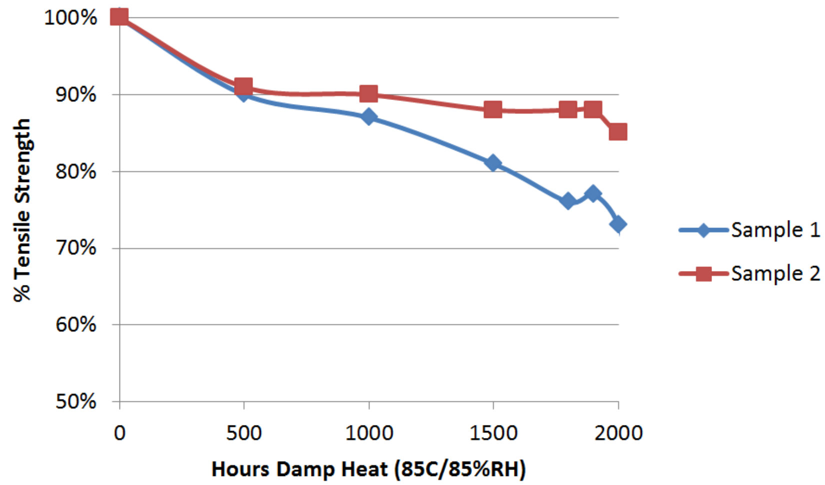

Figure 37: SunPower backsheet material tensile strength (normalized against its initial tensile strength) after exposure to damp heat for 2000 hours for different samples.

The literature on polymer hydrolysis is quite extensive. For example, McMahon finds that the tensile strength of PET drops linearly with the natural log of A/(A-x), where A/(A-x) is essentially a fraction of the backsheet that is hydrolyzed. Hydrolysis essentially cuts the polymer chains, weakening the polymer network. At some point, this reaches a critical point and tensile strength begins to drop more rapidly due to embrittlement – to only a few percent of its initial strength (Figure 38).

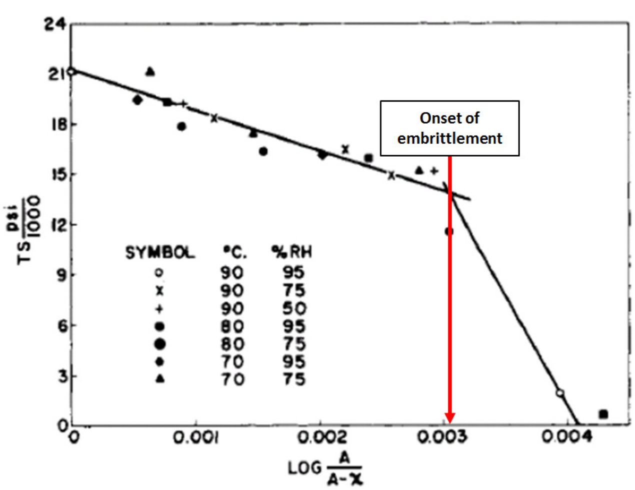

Figure 38: Loss of tensile strength versus hydrolyzed fraction, from McMahon [58]

SunPower conducts experiments similar to McMahon's approach in the qualification of new materials. Data sufficient to define curves, such as those shown above, and ascertain the value of A* = ln[A/(A-x)] at which the "onset of embrittlement" point is observed. In Figure 38, for example, this corresponds to A* = 0.0031.

For modeling, it is also important to understand dependence on temperature and relative humidity. Thus the parameter that must be computed at each time step is A*, via integration of the equation:

$$\frac{dA^*}{dt} = \mathrm{C}[\mathrm{H}]^{\mathrm{n}}\exp\left(-\frac{\mathrm{E_a}}{\mathrm{RT}}\right)$$

McMahon finds that C = exp(26.565), n = 0.99, and E_a = 25.7 kcal/mol. Here, [H] is the relative humidity (ranging from 0 to 1). Thus experiments are conducted at a variety of temperatures and typically at least two different levels of humidity. Generally the dependence on n is weak, so in the fitting of data it is often expedient (and supported by previous work) to assume n = 1.

SunPower is currently developing a statistical view of the likelihood of cracking; in the meantime PVLife conservatively defines the onset of this abrupt reduction of strength to a 100% chance of failure. This is conservative because typically at that point the backsheet material still maintains at least 60-65% of its initial strength. Based on these conservative criteria, it is found that SunPower backsheet materials are robust against this failure mode for well over 40 years (Figure 39) even in sub-tropical climates.

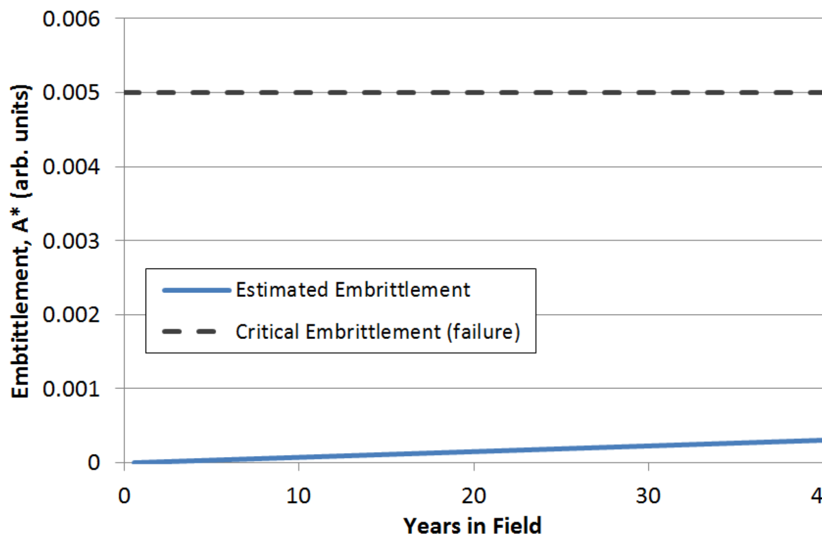

Figure 39: Backsheet degradation, based on experimental data fit to McMahon's model, shows sufficient backsheet strength for at least 40 years.

Note that PVLife computes the cell (and backsheet) temperature, which is what was used in this study, and which is considerably higher than ambient temperature. While this higher temperature of course tends to shorten the life of the backsheet, the effect is partially offset by the lower relative humidity (RH) (that is, the mass fraction of water is assumed to be the same near the surface as in ambient, but since the temperature is locally hotter, the local RH is lower, so the model is conservative).

Failure Mode: Solder-joint Failure

Solder joint fatigue is a dominant degradation mechanism in photovoltaic modules [7]. Modules in the field can experience temperature swings of up to 60°C per day; more if cells are reverse-biased. Due to mismatch in coefficients of thermal expansion (CTE) of the different materials in a module, these temperature changes create stresses between different materials (silicon, copper, glass). Dynamic mechanical action due to wind or snow load, as well as the occasional pressure exerted on the surface during shipping, installation, and maintenance, can also create internal stresses.

Solders are soft materials working relatively close to their melting temperature (in Kelvin) and are subject to creep under these internal stresses. Temperature cycles are more damaging than isothermal stresses of the same amplitude because of phase changes and solid-phase diffusions that happen at the same time. All these kneading actions on the solder material result in hardening and can eventually lead to cracks that propagate rapidly to relieve the build-in stress. Electrical failure follows mechanical failure, as parts that were joined by the solder become isolated from each other (Figure 40).

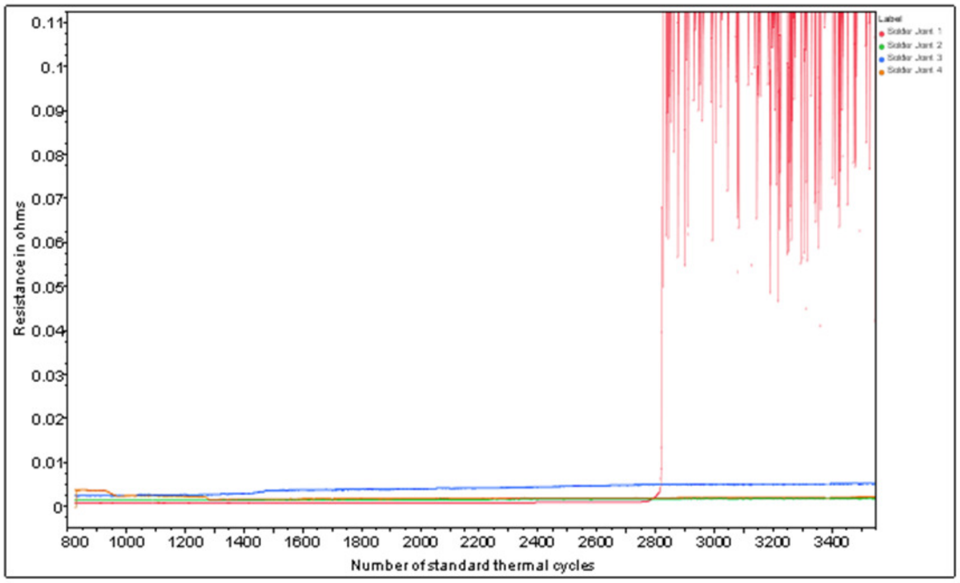

Figure 40: Electrical signature of a solder joint failure. Resistance can increase by many orders of magnitude. The red line shows a failing solder joint, while the other lines show joints which have not failed.

A failed solder joint in itself can seem benign as it is an open circuit that prevents any electrical energy to be transferred or dissipated. However, the moment of failure can be a dramatic event because solar cells are current sources. When a solder joint fails, its electrical resistance increases from nearly zero to an open circuit. With the cell as a current source, power increases as $P = R \times I^2$ with the voltage across the gap determined by the electrical topology of the rest of the solar field. This increase in power leads to an increase in temperature, to the point where metal can melt and air molecules can be ionized. Melting of the solder accelerates the failure of the joint, while the ionization can create a plasma in the newly formed air gap, sustaining a small electrical arc. This is why solder joint failures often result in burn marks through the module encapsulant and backsheet - the intense heat can also shatter the module glass and lead to further damage (Figure 41). For this reason, the study of solder joint integrity is of utmost importance for module reliability and safety.

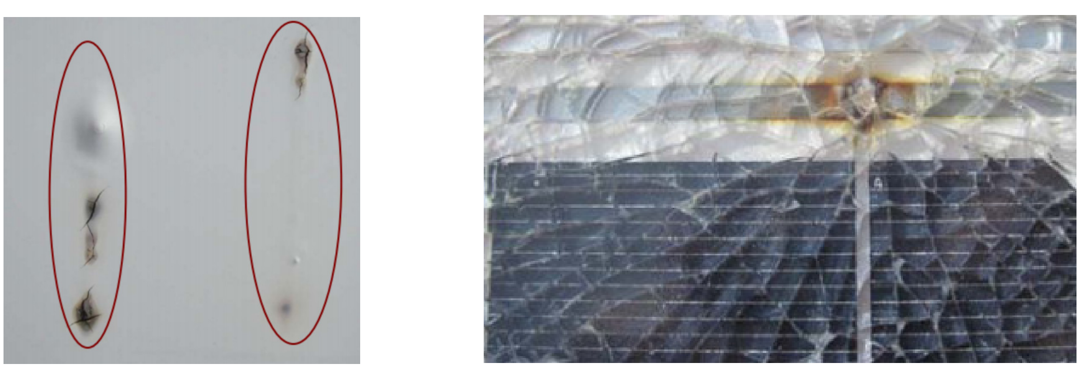

Figure 41: Thermal damage is an indicator of high solder joint resistance. When current is present, this resistance causes the joint to heat up. This heat can degrade performance or even cause module failure.

Examples show backsheet burns along the cell ribbons on a Conventional Module (left) and glass failure above the ribbon-bus bar joint on a Conventional Module (right) [62].

In order to characterize solder joint failure fail for SunPower modules, test structures were stressed through thermal cycling and dynamic load testing. Electron microscopy images were examined to identify whether the failure mechanism was due to the actual formation of voids or if brittle failure and intermetallic growth of Cu_3Sn were the cause. Void formation through grain boundary sliding and matrix creep were found to be the dominant failure modes (Figure 42).

Because these experiments take many years even with the maximum acceleration factor, it is difficult to get significant data with low uncertainty. Images from SEM did show a shift from failure at voids to brittle failure at intermetallic growth at temperatures over 90°C. Therefore the inclusion of intermetallic growth is important in hot climates or when considering chronically hot cells caused by shading or manufacturing defects.

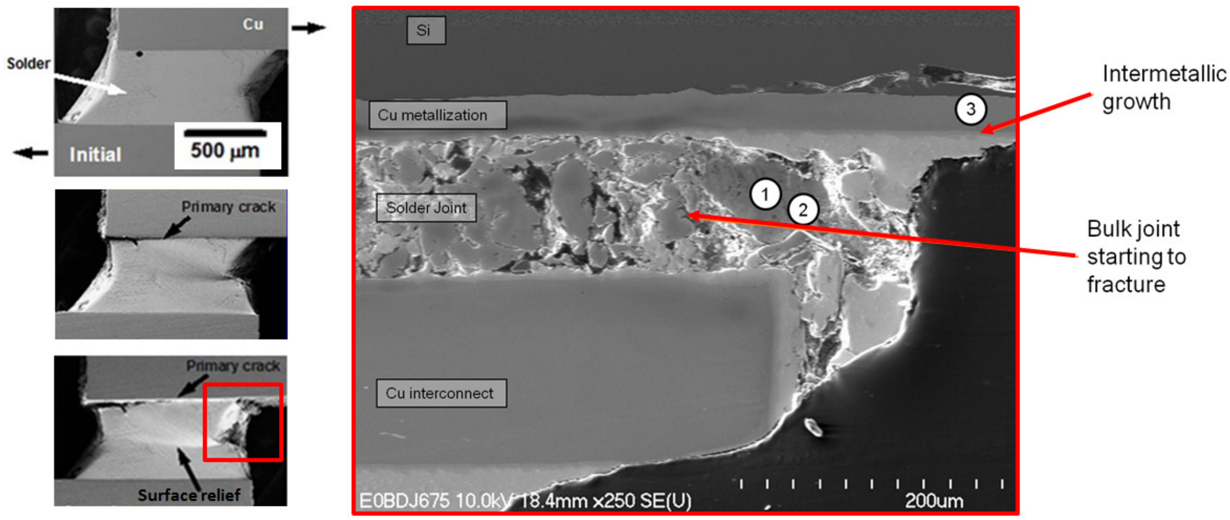

Figure 42: SEM images of solder joint on representative test structures show eventual solder joint failure through grain boundary sliding (1) matrix creep (2) and brittle intermetallic voiding (3).

SunPower worked with independent experts to model the stress-strain cycle for SunPower modules (Figure 43). The area of the stress-strain graph that this cycle describes represents the energy absorbed by the joint at each cycle. For each type of solder, there is a cumulated amount of energy a solder joint can absorb before it cracks. It is very difficult to measure this threshold of energy but the ratio of cycling energy between two different cycles is calculated, this threshold cancels out leaving the acceleration ratio between cycles.

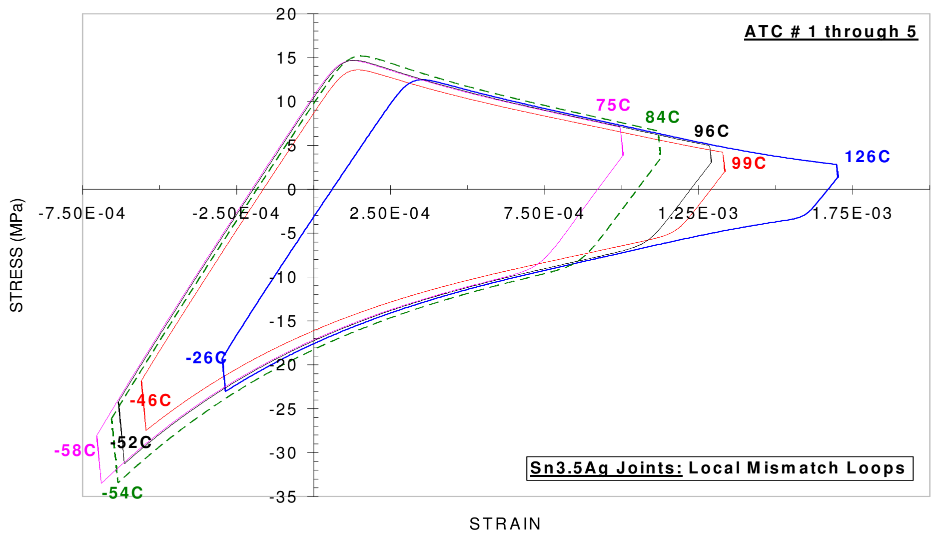

Figure 43: Strain energy is calculated from the stress-strain hysteresis loop for back-contact cells.

The area of the stress-strain curve for a dozen field conditions was calculated using weather data from different sites throughout the world. Also, the cycle was calculated for various laboratory conditions which differ in maximum temperature, temperature range, and ramp rate. All of these results were then fit to a model that allows extrapolation to expected conditions.

The result is an “acceleration factor calculator” which uses weather data for a given site, as well as parameters of a temperature profile in an environmental chamber, and calculates the acceleration factor (AF) between the two conditions. A key finding is that, in order to simulate 25 years of life in harsh desert conditions, 800 cycles of the standard thermal cycling test (-40℃ to +85℃) is needed. The difference between this and the traditional 200 cycle test used for certification underscores the point that certification tests are not necessarily representative of module reliability. It is important to note that the acceleration factor for solder joints between SunPower cells and the acceleration factor for a Conventional Module is very different because the design is different, as shown in Figure 10.

This study was complemented with three thermal cycling experiments with different temperature profiles. Using the failure time in these accelerated tests and the AF Calculator, the lifetime distribution of solder joints in any given environment can be determined. The model results in statistically 1 part per million modules failures due to solder joint failures (either from thermal cycling or intermetallic growth), and therefore the overall effective failure rate is <<1% in 25yrs and <1% at 40 years for one joint. Complete module failure, defined as point when the probability of three joints on one side of a cell failing is over 1% occurs beyond 70 years.

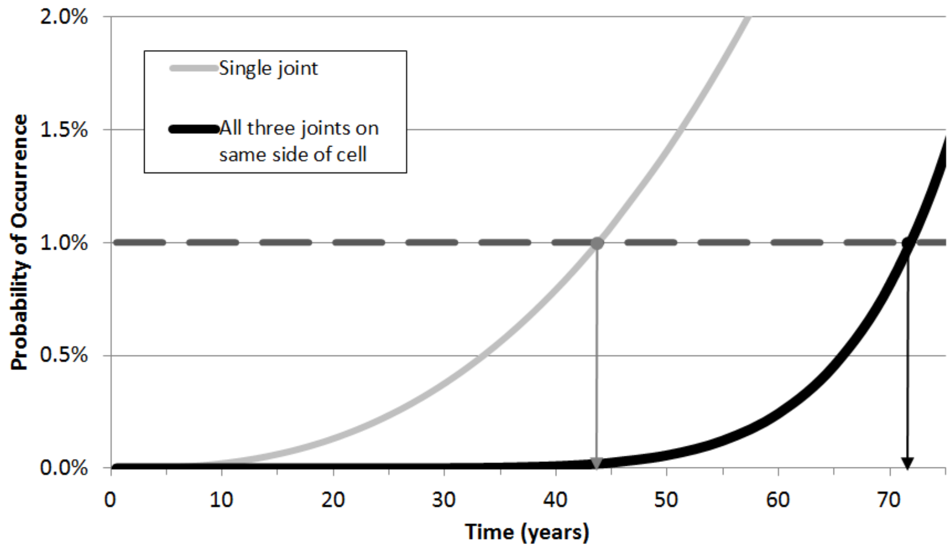

Figure 44: results of solder joint sub-model show that the probability of module failure exceeds the 1% threshold after 70 years. Module failure is defined as all three joints on one side of a side of a cell within a module failing.

Part III: A Side-by-Side Comparison of SunPower's Current and Previous Generation Modules

Bridging Generations

Part I of this white paper showed field data demonstrating a -0.32% per year median degradation rate for the previous generation of modules. Part II showed a detailed physical model for all the known degradation and failure rates, PVLife, and a summary of lab results on specific degradation modes. A key finding in Part II was that the vast majority of that 0.32% per year degradation in the generation of modules is due to three key modes: encapsulant photothermal yellowing, cell UV degradation, and polarization. In 2011 SunPower introduced its current technology, which effectively cuts photothermal yellowing in half and polarization to nearly zero. Using updated experimental and field data, the current generation was analyzed with PVLife, resulting in an average degradation rate off less than 0.25% per year (Figure 21).

This section presents a battery of side-by-side accelerated tests that show the current generation of modules is superior to previous generation in several regards that not only improve degradation but also increase module lifetime. These improvements are reflected in a variety of PVLife simulations in various climates.

UV Degradation

As described previously, SunPower has designed out many of the degradation modes that affect Conventional Modules. Encapsulant yellowing remains as the largest contributor to degradation – and in SunPower's previous generation of modules, about half of the power degradation was due to encapsulant yellowing. As encapsulant browns it transmits less light, leading to less current generation. SunPower has spent many years developing and qualifying an improved encapsulant formulation that better resist the creation of absorbing chromophores. SunPower has reduced the effect of this mode by more than half.

The chemical kinetics of this degradation mode was summarized in Part II; recall that the reaction pathway that creates absorbing chromophores is driven by temperature and high energy (UV) photons. In order to compare SunPower's current generation of modules to the previous generation, pure temperature effects are investigated. Coupons (mini-laminates of 3 cells) were exposed to dry heat for 90 days at 100ºC, 120ºC, and 130ºC. These temperatures are much higher than normally experienced in the field but are reasonable for accelerated testing. Short circuit current, I_{sc}, was periodically measured to determine the transmission loss. Results of this temperature dependency experiment are shown in Figure 45. The previous generation incurred increasing power degradation with higher temperatures and exposure time. Meanwhile, the current generation showed no appreciable power loss and no visible change in color at all temperatures for the duration of the test, even at the hottest temperature (130ºC).

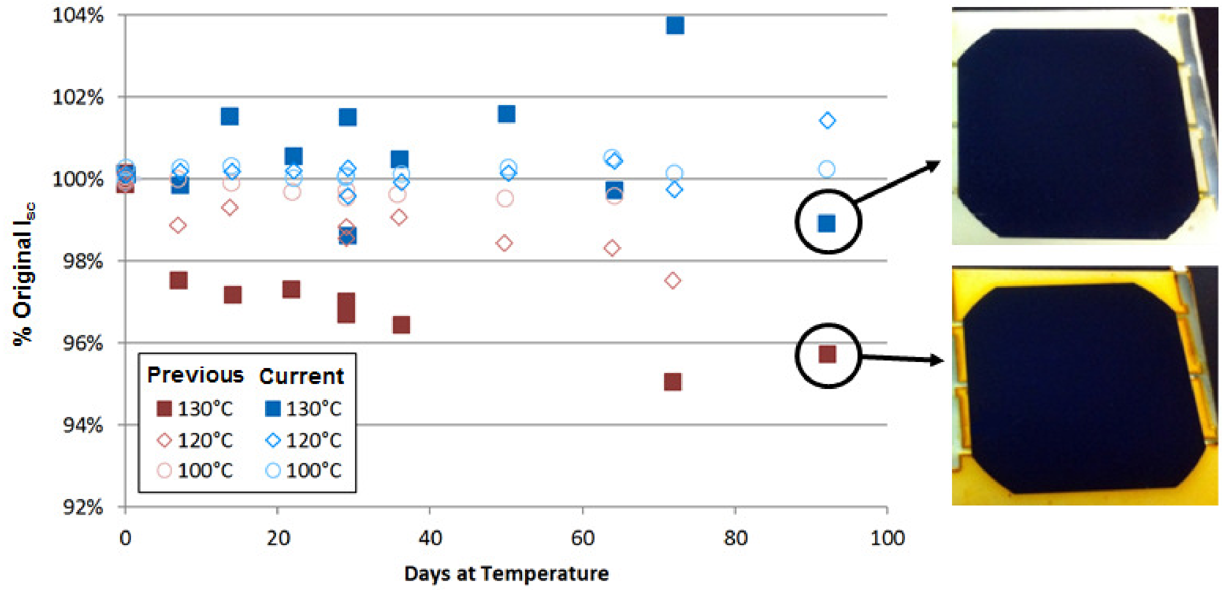

Figure 45: Change in Isc over time. The current generation (blue) shows minimal power loss and discoloration, such that results are within instrument noise; previous generation (red) shows substantial browning after 90 days at both 120^{0}C and 130^{0}C.

In a different experiment, coupons were exposed to a combination of elevated temperatures of 50ºC, 80ºC, and 110ºC and high intensity UV light (25X 1-sun irradiance between 300 nm and 400 nm wavelengths) for 850 hours. Transmission and I_{sc} were periodically measured.

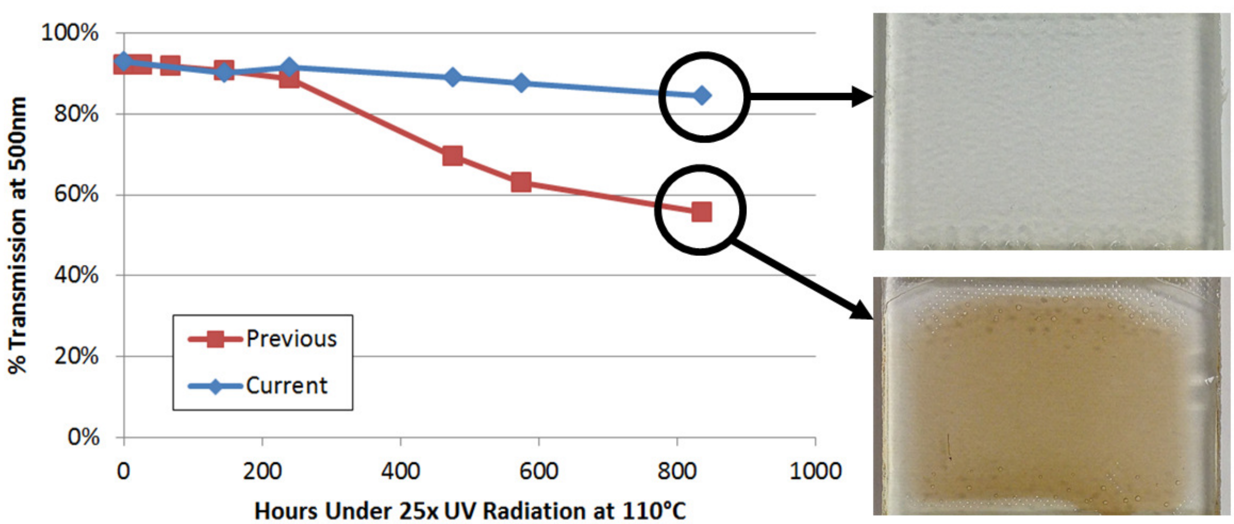

Figure 46: Change in transmission at 500nm for previous (red) and current (blue) generations at twenty five times UV radiation exposure and elevated temperature. The current generation has almost three times slower degradation at this wavelength.

Results show that the transmission loss of the current generation is up to five times slower than the previous generation, depending on temperature. For example, Figure 46 shows the transmission at 500 nm. After 575 hours at 110 ℃, the previous generation falls from 92% to 63% (0.05%/hour), while the current generation only to 93% to 88% (0.01%/hour). Even after 850 hours, as the degradation of the previous generation begins to level off, the current generation has less than one quarter of the degradation.

Electrical Leakage and Polarization/HVD/Potential-Induced Degradation

As discussed previously, SunPower's previous generation was susceptible to polarization and HVD, and required positive grounding. SunPower has made changes to the design to eliminate these degradation modes, allowing the modules to have a positive, negative, or floating ground for the current generation. The design is also highly resistant to potential induced degradation (PID) in all grounding configurations.

Three field and lab tests demonstrate this resistance to voltage stresses. First, in order to characterize positive and negative grounding on the current generation, two separate strings of modules were installed in both grounding configurations in a hot and humid climate (a hot and humid climate is a good driver of electro-chemical degradation). Weekly production was recorded for each string and the data shows that there is not a significant difference in production between the two configurations (Figure 47).

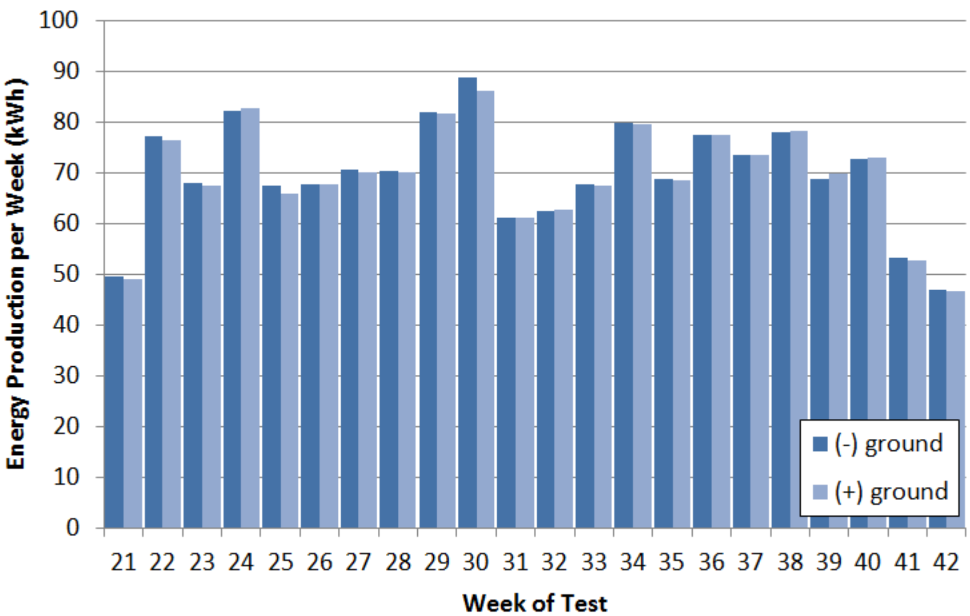

Figure 47: Outdoor test results comparing negative and positive-grounded current generation SunPower modules in a humid climate (Philippines). In the previous generation, positive grounding was necessary to prevent a reversible but significant drop in performance. In the current generation, there is no significant difference in performance.

In another outdoor experiment, SunPower conducted a test in which modules were subjected to continuous water spray and 5000V bias with negative grounding for 18 weeks. The water spray presents a worst-case condition, since the entire glass surface is grounded, maximizing the leakage current. Results show a 1% drop in module power and a 1% drop in V_{oc} (Figure 48). V_{oc} is especially pertinent in this case because it is an indication of actual cell degradation removed from test artifacts. Test artifacts, such as contaminants in the chamber which cause glass hazing, can affect measurements; but, cleaning is not a regular part of the IEC testing protocol.

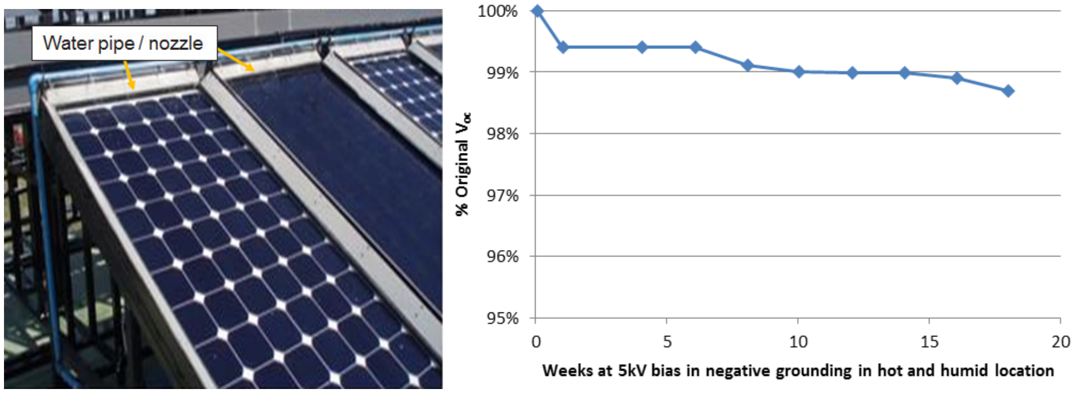

Figure 48: Outdoor test results on a module with 5kV applied to the cells in negative grounding with continuous water spray applied in Manila, Philippines for 18 weeks.

Electro-chemical degradation can also be observed in the laboratory through damp heat with bias testing. Modules are placed in a damp heat chamber and a voltage bias is applied to the module. Due to the recent focus on PID within academia and the market, this stress is currently being considered as part of mandatory module certification. While the test procedure is still in draft, the current version (IEC 62804) currently calls for 60^0C at 85%RH for 96 hours. Koch has shown that testing at 60^0C is half as severe as testing at 85^0C for a given number of hours [63].

SunPower conducts damp heat with bias testing at 85^0C, 85% relative humidity, and 1000V bias. In one experiment, module leads were connected to +1000V and the frame was connected to negative ground for 1000 hours. The module was periodically removed from the chamber, placed outdoors for a day to control for test artifacts, and measured. Power (module efficiency) dropped 3% after 1000 hours at 85^0C. In addition, electroluminescence images and a 0% V_{oc} drop post aging indicate that the cells were not damaged during the test (Figure 49).

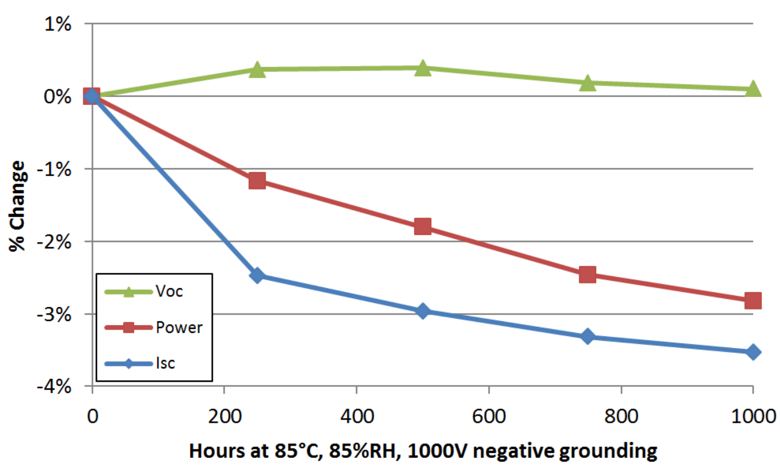

Figure 49: Laboratory damp heat with bias tests for polarization/HVD/PID. Module is subjected to 85^0C/85%RH for 1000 hours with 1000V applied to cells in negative grounding configuration.

External studies are consistent with these findings. In a recent study by the Fraunhofer Institute [64], modules were tested at 85^0C/85%RH for 400 hours. The power on Conventional Modules degraded up to 25% within the first 50 hours, while SunPower modules showed less than 2% degradation for both grounding configurations.

Interestingly, the degradation of Conventional Modules varies widely, likely due to the differences in the design, processing, or materials. In a second study [63], the power on Conventional Modules was tested at 85^{o}C/85%RH for 48 hours. The modules degraded by 3-40%, even after a thermal assisted recovery. Thermal annealing and changing the string bias are two ways to reverse some of the effects of PID and often discussed in literature; however, these solutions only work for some degradation modes, and are not necessarily practical for a fielded unit.

Moisture-driven degradation

As discussed in Part I, moisture can have deleterious effects on cell and module performance, but SunPower's cells and modules minimize these effects. Recall that Figure 12 in Part I shows damp heat results for SunPower and Conventional Modules and demonstrates that both previous and current generation SunPower modules have significantly lower degradation. In a second side-by-side test, current and previous generation modules were exposed to the same extended IEC61215 damp heat tests. The current generation showed V_{oc} degradation that is approximately seven times slower than the previous generation (Figure 50). V_{oc} drop indicates actual cell degradation, showing that SunPower's current generation is resistant at the cell level. Note that much of the efficiency was recovered after cleaning the front glass surface, indicating that this is an artifact of water in the test chamber.

In short, while SunPower's previous generation modules have a very low degradation rate compared to Conventional Modules, SunPower's current generation essentially eliminates this degradation mode entirely. Note that DH is one of the most frequently-failed certification tests – it is "one of the most difficult tests for companies to pass" [3], and recent work by NREL [20] indicates that 2000-3000 hours of DH roughly corresponds to 20 years in a tropical environment. This implies that current IEC 61215 certification requirement of 1000 hours leaves a safety factor that is less than unity.

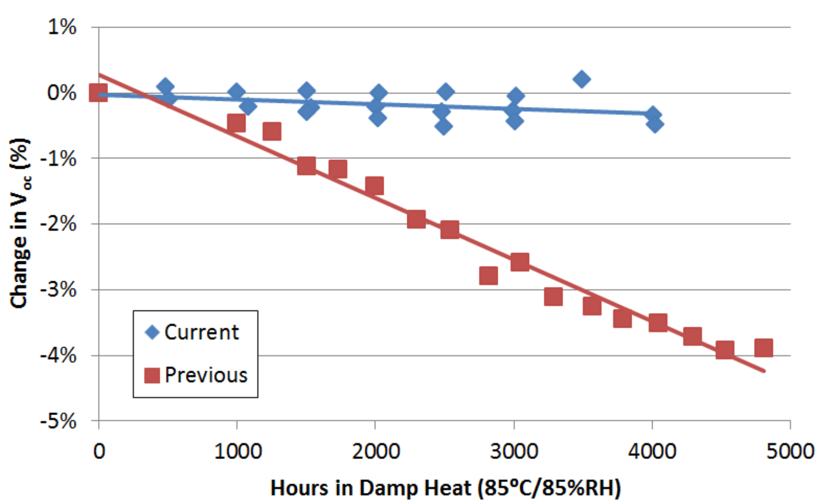

Figure 50: Change in efficiency and Voc with exposure to damp heat. The current generation platform shows approximately one seventh the degradation rate of the previous generation using linear fits.

Humidity Freeze Testing

Finally, side-by-side comparisons of SunPower's current and previous generation were performed in extended humidity freeze (HF) cycling tests for. In humidity freeze, modules are soaked in damp heat (85C, 85% relative humidity) for twenty hours, which effectively saturates the modules with moisture. The temperature is then dropped to -40°C for thirty minutes to freeze the water. The freezing water expands, stressing weak points within the laminate and cells. The moisture exposure followed by freezing makes this test is particularly good for testing for degradation modes such as A/R glass robustness and delamination with subsequent moisture ingress [38]. Humidity freeze for ten cycles is used by IEC, UL, TUV, JET, CSA, and other certification agencies.

SunPower has tested its current generation above HF300, at which point the power remains above 95%, and its previous generation to HF280, at which point the power remains above 90% (Figure 51). In contrast over 10% of Conventional Modules submitted since 2005 to TUV for design qualification testing (HF10) failed HF10 with more than 5% power loss [65].

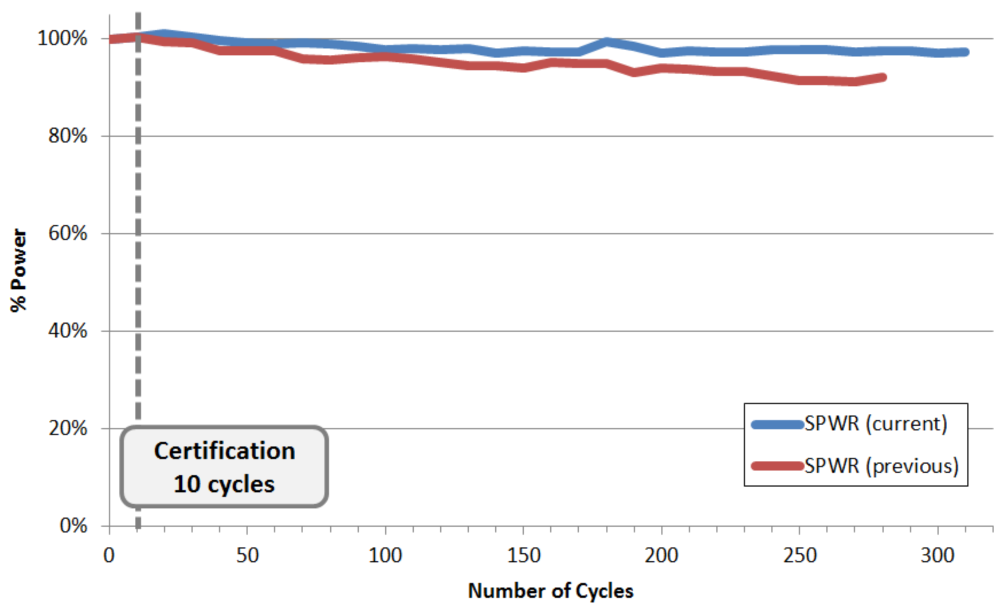

Figure 51: SunPower shows minimal degradation after two hundred eighty humidity-freeze cycles.

Summary: Enhanced SunPower Reliability

A list of the comparisons performed and relative performance is summarized below. These tests show that major degradation modes of the previous technology have been eliminated or significantly reduced on the current generation of SunPower modules.

Table 3: Comparative data between previous and current generations of SunPower modules

Degradation Mode	Test	Current versus Previous
Transmission/Isc Loss	Thermal Yellowing	Current had no degradation
	UV induced degradation	2-8x slower degradation rate
	Cu catalyzed yellowing	Current had no degradation
Electrical Stress	Polarization stresses	Current can be grounded in (+) or (-) configuration
Power and Voltage loss	Damp heat	7x slower degradation rate
	Humidity freeze	3x slower degradation rate

Conclusion

In section 2, it was shown that PVLife agrees well with observed fleet-average degradation rates for SunPower's previous generation (Figure 22), so it is reasonable to modify the model to assess the impact of these changes for SunPower's current generation. To support this effort, major degradation modes (cell and encapsulant UV, polarization) and failure modes (backsheet delamination and solder joint failure) were quantitatively assessed as described in Part II of this white paper and applied within the PVLife physical model in the same way as the previous generation. Activation energies and other rate constants for encapsulant yellowing, additional cell UV experiments, and polarization tests have been conducted on the current generation to obtain updated model parameters. The model was then used to simulate module performance at three key climates using historical weather and irradiance data: Phoenix, AZ (representing a hot and dry climate) and Miami, FL (representing a hot and humid climate), and San Jose, CA (representing a temperate climate).

The degradation in a harsh desert climate is shown below in Figure 52. The dramatic improvement in encapsulant yellowing and polarization is readily apparent, as is a slight tradeoff of increased UV degradation at the cell level. For example, in hot/dry climates, over 25 years the encapsulant yellowing impact on performance is reduced by 6.4% while UV impact increases 1.2%and polarization essentially disappears, improving average 25-year degradation from 5.9% to 3%. In this climate, current generation of SunPower modules degrades at about half the rate of the previous generation.

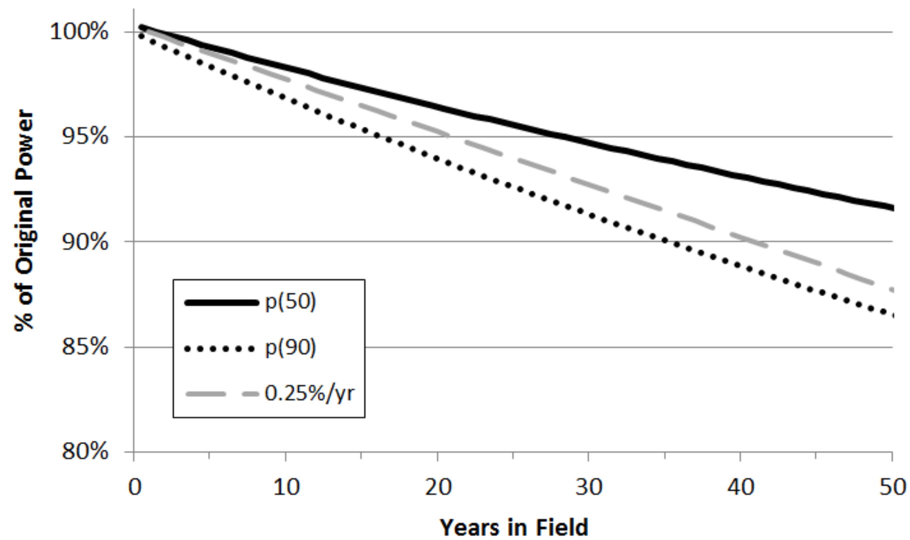

Figure 52: PV Life output for the current generation of Maxeon cells (black) in a utility installation and a desert climate. Lower 90% confidence level (black dashed) reflects the combined uncertainties from degradation modes. Module starting point is offset to match mean module power distribution above nameplate rating. Based on current modeling, an average module is expected to degrade less than 0.25% per year.

SunPower modules have a fundamentally different design and materials which provide superior reliability in real world conditions. Primary failure modes which affect standard efficiency conventional cells have been designed out of SunPower's cells, while other design and manufacturing differences ensure robustness against the effects of humidity, temperature changes, dynamic loading, and shading. Qualification of materials is performed via extended qualification tests well beyond industry standards, and based on the physics of failure modes rather than just standardized tests, resulting in a module that outperforms in practically every stress test available.

SunPower's cell design is based on decades of applied research and development. The fundamental physics of key degradation modes have been studied in detail and quantified via modeling of encapsulant browning, cell UV degradation, voltage stress, and several failure modes. This research has resulted in PVLife, a holistic performance degradation model which has been validated with real-world data from the field, including a study conducted on 3.2 million module-years of data for SunPower's previous generation modules.

Systematic enhancements that have reduced or eliminated the top two degradation modes SunPower's previous generation, backed by extensive qualification testing and additional characterization, demonstrate that the current generation has even lower degradation rates. These data and validated physical models result in an expected degradation rate of <0.25% per year for SunPower's current generation modules.

Appendix A

Estimates of Degradation Rates for Conventional Modules from Field Studies

There is no consensus number for the annual degradation of conventional crystalline modules; however, it has been the focus of academic study for years. Various field studies have measured the degradation rate of Conventional Modules and they indicate a degradation rate of approximately -1.0% per year. Key studies and descriptions follow:

- Sample, T. (2011). Failure Modes and Degradation Rates from Field-Aged Crystalline Silicon Modules. In *PV Module Reliability Workshop,* Golden, CO.

  This degradation study includes 204 c-Si modules from 20 manufacturers. Modules were fielded in northern Italy (moderate temperature, high humidity) for 18-20 years. The average degradation is -1.0% per year.

- Jordan, D. C., & Kurtz, S. R. (2013). Photovoltaic Degradation Rates — an Analytical Review. *Progress in Photovoltaics: Research and Applications*, *21*, 12–29. doi:10.1002/pip

  Jordan and Kurtz review existing literature on degradation rate. He synthesizes nearly 2000 degradation rates from around the world, covering over 40 years of data. For c-Si modules, the average degradation rate is -0.7% per year.

- Suleske, A. A. (2010). *Performance Degradation of Grid-Tied Photovoltaic Modules in a Desert Climatic Condition*. Arizona State University.

  Suleske investigates the performance of approximately 1,900 grid-tied c-Si modules installed in the Arizona desert for 10-17 years. The average degradation rate is -1.5% per year.

- Pulver, S., Cormode, D., Cronin, A., Jordan, D., Kurtz, S., & Smith, R. (2010). Measuring Degradation Rates Without Irradiance Data. In *IEEE Photovoltaic Specialists Conference, 35th*.

  Pulver, et al, measure degradation rate on 22 grid-tied PV systems in Tucson, Arizona. The silicon modules are 3-5 years old and exhibit an average degradation rate of 1.1% per year.

- Vázquez, M., & Rey-Stolle, I. (2008). Photovoltaic Module Reliability Model Based on Field Degradation Studies. *Progress in Photovoltaics: Research and Applications*, *16*(5), 419–433. doi:10.1002/pip.825

  Vasquez and Rey-Solle explore modeling degradation rate. As part of this research, they analyze several relatively temperate sites around the world. The c-Si modules using EVA as encapsulant are fielded from 1.5 to 22 years and have an average degradation rate of 0.8 per year %

SunPower has conducted a large study on its own fleet. The study includes 179 systems (42 MW) using Conventional Modules as old as 11.5 years. Data spanning back to the site commissioning date were used to determine fleet-wide degradation rates, representing 3.2 million module-years of monitored data. The annual system power degradation rate (including inverter) for Conventional Systems were found to degrade at -1.25 ± 0.25% (95% confidence) per year, and in both cases were shown to be linear with time.

The National Renewable Energy Laboratory (NREL) in Golden, Colorado, has installed SunPower's previous generation of module in an outdoor test facility, where it has degraded at a rate of less than 0.1% per year [69]; however, this site represents a relatively mild climate due to the cool temperature and low humidity. As discussed above, SunPower recommends an average system degradation rate of

0.25% per year for SunPower's current technology to account for different climates and deployment conditions.

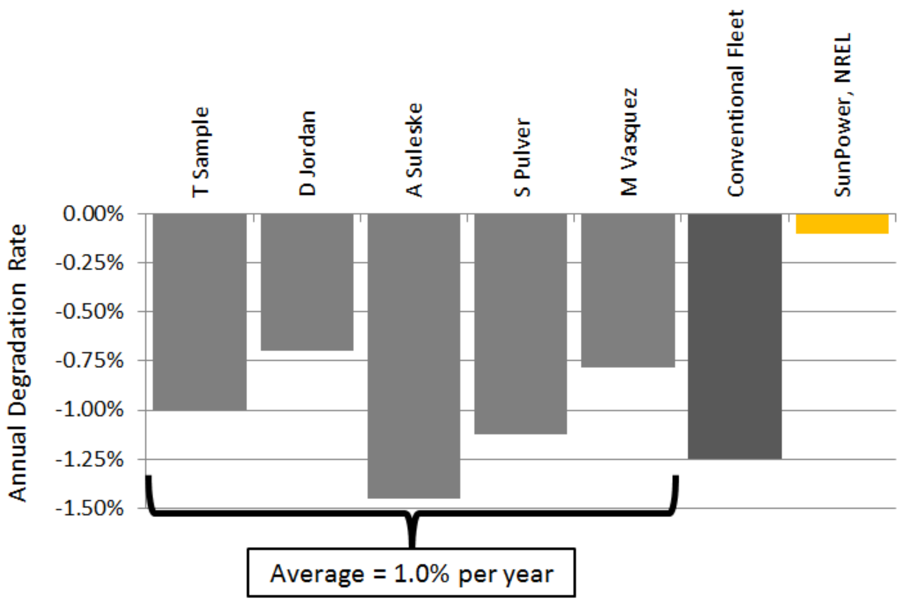

Figure 53: Summary of average annual degradation rates from independent studies. Average value for Conventional Modules is -1.0% per year. SunPower's study of its third party fleet indicates a -1.25% per year degradation rate. Previous generation SunPower modules installed at NREL's test yard show a 0.1% annual degradation rate.

Bibliography

[1] C. R. Osterwald and T. J. Mcmahon, "History of Accelerated and Qualification Testing of Terrestrial Photovoltaic Modules : A Literature Review," *Progress in Photovoltaics: Research and Applications*, vol. 17, pp. 11–33, 2009.

[2] J. Lathrop, C. Davis, and E. Royal, "An Accelerated Stress Testing Program For Determining The Reliability Sensitivity Of Silicon Solar Cells To Encapsulation And Metallization Systems," in *IEEE Photovoltaic Specialists Conference, 16th*, 1982, pp. 1262–1267.

[3] G. Tamizhmani, B. Li, T. Arends, J. Kuitche, B. Raghuraman, W. Shisler, K. Farnsworth, A. Voropayev, D. Parker, and T. U. V. R. Ptl, "Failure Analysis Of Module Design Qualification Testing - III: 1997-2005 vs. 2005-2007 vs. 2007-2009," in *IEEE Photovoltaic Specialists Conference, 35th*, 2010, pp. 251–255.

[4] J. H. Wohlgemuth, "History Of IEC Qualification," in *International PV Module QA Forum*, 2011.

[5] K. Kato, "PV Module Failures Observed In The Field 'PVRessQ!'," in *PV Module Reliability Workshop*, 2012.

[6] J. H. Wohlgemuth, D. Cunningham, A. Nguyen, and J. Miller, "Long Term Reliability of PV Modules," in *European Photovoltaic Solar Energy Conference and Exhibition, 20th*, 2005, no. June, pp. 6–10.

[7] J. H. Wohlgemuth, "Reliability of PV Systems," *Proceedings of SPIE2*, vol. 7048, p. 704802.

[8] T. Sample, "Failure Modes and Degradation Rates from Field-Aged Crystalline Silicon Modules," in *PV Module Reliability Workshop*, 2011, no. February, pp. 1–31.

[9] D. C. Jordan and S. R. Kurtz, "Photovoltaic Degradation Rates — an Analytical Review," *Progress in Photovoltaics: Research and Applications*, vol. 21, pp. 12–29, 2013.

[10] A. A. Suleske, "Performance Degradation of Grid-Tied Photovoltaic Modules in a Desert Climatic Condition," Arizona State University, 2010.

[11] S. Pulver, D. Cormode, A. Cronin, D. Jordan, S. Kurtz, and R. Smith, "Measuring Degradation Rates Without Irradiance Data," in *IEEE Photovoltaic Specialists Conference, 35th*, 2010, no. February.

[12] M. Vázquez and I. Rey-Stolle, "Photovoltaic Module Reliability Model Based on Field Degradation Studies," *Progress in Photovoltaics: Research and Applications*, vol. 16, no. 5, pp. 419–433, Aug. 2008.

[13] M. Anderson and Z. Defreitas, "A SunPower Fleet-Wide System Degradation Study using Year-over-Year Performance Index Analysis," 2012.

[14] J. Wendt, M. Träger, M. Mette, A. Pfennig, and B. Jaeckel, "The Link Between Mechanical Stress Induced By Soldering And Micro Damages In Silicon Solar Cells," in *European Photovoltaic Solar Energy Conference and Exhibition, 24th*, 2009, pp. 3420–3423.

[15] R. Meier, F. Kraemer, S. Wiese, K. Wolter, J. Bagdahn, P. Csp, and H. Saale, “Reliability Of Copper-Ribbons In Photovoltaic Modules Under Thermo-Mechanical Loading,” in *IEEE Photovoltaic Specialists Conference, 35th*, 2010, pp. 1283–1288.

[16] N. Bosco, “Modeling Metal Fatigue As a Key Step in PV Module Life Time Prediction outline • Modeling metal fatigue,” in *PV Module Reliability Workshop*, 2012.

[17] T. Adcock, “Lower Cost , Greater Efficiency Drive Back- contact Solar Module Dev,” *renewableenergyworld*, 2011. [Online]. Available: http://www.renewableenergyworld.com/rea/news/article/2011/06/lower-cost-greater-efficiency-drive-back-contact-solar-module-dev. [Accessed: 07-Feb-2013].

[18] L. Abra, S. B. Rim, S. D. Kim, S. Corporation, S. Jose, and U. States, “Temperature of Solder Contact in Back-Contact Si Solar Cells and Its Effect on Reliability of Modules under Localized Shading Environments,” in *IEEE Photovoltaic Specialists Conference, 38th*, 2012, no. 1.

[19] B. Ketola and A. Norris, “Degradation Mechanism Investigation of Extended Damp Heat Aged PV Modules,” in *European Photovoltaic Solar Energy Conference and Exhibition, 26th*, 2011, pp. 3523–3528.

[20] M. Kempe, J. Wohlgemuth, D. Miller, M. Reese, and A. Dameron, “Modeling the Ranges of Stresses for Different Climates / Applications,” in *International PV Module QA Forum*, 2011.

[21] U. Jahn and T. Ü. V Rheinland, “PV Module Reliability Issues Including Testing And Certification,” in *European Photovoltaic Solar Energy Conference and Exhibition, 27th*, 2012, no. September.

[22] M. Köhl, K. Weiss, M. Heck, and D. Philipp, “PV reliability : Results of a German four-year joint project Part I : accelerated ageing tests and modelling of degradation,” in *European Photovoltaic Solar Energy Conference and Exhibition, 24th*, 2009.

[23] P. Grunow, S. Lust, and D. Sauter, “Weak light performance and annual yield of PV modules and systems as a result of the basic parameters set of industrial solar cells,” *… Photovoltaic Solar …*, 2004.

[24] J. H. Wohlgemuth and S. R. Kurtz, “How Can We Make PV Modules Safer?,” no. June, 2012.

[25] M. Petzold, C. Dresbach, M. Ebert, J. Bagdahn, M. Wiemer, K. Glien, J. Graf, R. Müller-Fiedler, and H. Höfer, “Fracture mechanical life-time investigation of glass frit-bonded sensors,” in *Thermal and Thermomechanical Proceedings 10th Intersociety Conference on Phenomena in Electronics Systems*, 2006, pp. 1343–1348.

[26] S. Pingel, Y. Zemen, and O. Frank, “Mechanical stability of solar cells within solar panels,” *Proc. of 24th …*, 2009.

[27] H. Wirth, “Solder joint formation and testing on cell busbars,” in *Workshop on Metallization for Crystalline Silicon Solar Cells, 2nd*, 2010.

[28] J. H. Wohlgemuth, “IEC 61215: What It Is and Isn’t,” in *PV Module Reliability Workshop*, 2012.

[29] P. Chaturvedi, B. Hoex, and T. M. Walsh, “Broken metal fingers in silicon wafer solar cells and PV modules,” *Solar Energy Materials and Solar Cells*, vol. 108, pp. 78–81, Jan. 2013.

[30] K. Bothe, K. Ramspeck, D. Hinken, C. Schinke, J. Schmidt, S. Herlufsen, R. Brendel, J. Bauer, J.-M. Wagner, N. Zakharov, and O. Breitenstein, "Luminescence emission from forward- and reverse-biased multicrystalline silicon solar cells," *Journal of Applied Physics*, vol. 106, no. 10, p. 104510, 2009.

[31] F. Fertig, S. Rein, M. Schubert, and W. Warta, "Impact Of Junction Breakdown In Multi-Crystalline Silicon Solar Cells On Hot Spot Formation And Module Performance," in *European Photovoltaic Solar Energy Conference and Exhibition, 26th*, 2011, no. September.

[32] O. Breitenstein, J. Bauer, K. Bothe, W. Kwapil, D. Lausch, U. Rau, J. Schmidt, M. Schneemann, M. C. Schubert, J.-M. Wagner, and W. Warta, "Understanding junction breakdown in multicrystalline solar cells," *Journal of Applied Physics*, vol. 109, no. 7, p. 071101, 2011.

[33] J. Schmidt, "Light-Induced Degradation in Crystalline Silicon Solar Cells," *Solid State Phenomena*, vol. 95–96, pp. 187–196, 2004.

[34] J. Schmidt and R. Hezel, "Light-Induced Degradation In Cz Silicon Solar Cells : Fundamental Understanding And Strategies For Its Avoidance," in *Workshop on Crystalline Silicon Solar Cell Materials and Processes, 12th*, 2002, no. August, pp. 1–8.

[35] T. Saitoh, H. Hashigami, S. Rein, and S. Glunz, "Overview of light degradation research on crystalline silicon solar cells," *Progress in Photovoltaics: Research and Applications*, vol. 8, no. 5, pp. 537–547, 2000.

[36] R. Crabb, "Proceedings of the 9th PVSC," 1972, p. 329.

[37] S. W. Glunz, S. Rein, J. Y. Lee, and W. Warta, "Minority carrier lifetime degradation in boron-doped Czochralski silicon," *Journal of Applied Physics*, vol. 90, no. 5, p. 2397, 2001.

[38] S. Kurtz, J. Granata, and M. Quintana, "Photovoltaic-Reliability R & D Toward a Solar-Powered World," in *Proceedings of SPIE*, 2009, vol. 7412.

[39] M. A. Mikofski, D. F. J. Kavulak, D. Okawa, Y. Shen, A. Terao, M. Anderson, S. Caldwell, D. Kim, N. Boitnott, J. Castro, L. Ann, L. Smith, R. Lacerda, D. Benjamin, and E. Hasselbrink, "PVLife : An Integrated Model for Predicting PV Performance Degradation over 25 + Years," in *IEEE Photovoltaic Specialists Conference, 38th*, 2012, no. 3, pp. 1744–1749.

[40] M. Mikofski, M. Anderson, S. Caldwell, D. Degraaff, E. Hasselbrink, D. Kavulak, R. Lacerda, D. Okawa, Y. Shen, A. Tedjasaputra, A. Terao, and Z. Xie, "A Dynamic Cell-by-Cell PV System Model to Predict Lifetime Performance and Reliability," in *European Photovoltaic Solar Energy Conference and Exhibition, 26th*, 2011.

[41] E. F. C. Hasselbrink, D. Ph, C. Mark, D. F. J. Kavulak, D. Okawa, Y. Shen, A. Terao, M. Anderson, W. Caldwell, D. Kim, N. Boitnott, L. Ann, L. Smith, and R. Lacerda, "Module Lifetime Prediction through Integrated Modeling of Known Failure Modes," in *PV Module Reliability Workshop*, 2012, pp. 1–18.

[42] D. L. King, W. E. Boyson, and J. A. Kratochvill, "Photovoltaic Array Performance Model," 2004.

[43] NREL, "Bird Simple Spectral Model: spectrl2." [Online]. Available: http://rredc.nrel.gov/solar/models/spectral/spectrl2/. [Accessed: 21-Feb-2013].

[44] NASA, "US Standard Atmosphere, 1976," Washington, D.C., 1976.

[45] D. L. King, S. Gonzalez, G. M. Galbraith, and W. E. Boyson, “Performance Model for Grid-Connected Photovoltaic Inverters,” 2007.

[46] S. Gonzalez, S. Kuszmaul, and A. Ellis, “Long-term inverter operation demonstration at Sandia National Laboratories,” *… Conference (PVSC), 2009 …*, pp. 1937–1942, 2009.

[47] R. a. Sinton and R. M. Swanson, “Recombination in highly injected silicon,” *IEEE Transactions on Electron Devices*, vol. 34, no. 6, pp. 1380–1389, Jun. 1987.

[48] R. Fischer and W. Ketola, *Accelerated and Outdoor Durability Testing of Organic Materials*. Material Park: ASTM International, 1994, pp. 88–111.

[49] J. F. Rabek, *Polymer Photodegradation: Mechanisms and Experimental Methods*, 1st ed. Chapman & Hall, 1995.

[50] J. H. Wohlgemuth and S. Kurtz, “Using accelerated testing to predict module reliability,” in *IEEE Photovoltaic Specialists Conference, 37th*, 2011, pp. 1–5.

[51] a. W. Czanderna and F. J. Pern, “Encapsulation of PV modules using ethylene vinyl acetate copolymer as a pottant: A critical review,” *Solar Energy Materials and Solar Cells*, vol. 43, no. 2, pp. 101–181, Sep. 1996.

[52] R. Swanson, M. Cudzinovic, D. Deceuster, V. Desai, J. Jürgens, N. Kaminar, W. Mulligan, D. Rose, D. Smith, A. Terao, K. Wilson, S. Corporation, and I. Way, “The Surface Polarization Effect In High- Efficiency Silicon Solar Cells,” in *IEEE Photovoltaic Specialists Conference, 15th*, 2005, pp. 1–4.

[53] R. Swanson, D. DeCeuster, V. Desai, D. Rose, D. H. Smith, and N. Kaminar, “Preventing Harmful Polarization of solar Cells,” 7,554,031 B22009.

[54] P. Hacke, K. Terwilliger, R. Smith, S. Glick, J. Pankow, M. Kempe, S. Kurtz, I. Bennett, and M. Kloos, “System Voltage Potential- Induced Degradation Mechanisms in PV Modules and Methods for Test Preprint,” in *IEEE Photovoltaic Specialists Conference, 37th*, 2011, no. July.

[55] D. J. Dimaria, D. Arnolda, T. J. Watson, P. O. Box, Y. Heights, and N. York, “Impact ionization , trap creation , degradation , dioxide films on silicon and breakdown in silicon,” *Journal of Applied Physics*, vol. 73, no. 7, pp. 3367–3384, 1993.

[56] Y. Park and D. Schroder, “Degradation of thin tunnel gate oxide under constant Fowler-Nordheim current stress for a flash EEPROM,” *IEEE Transactions on Electron Devices*, vol. 45, no. 6, pp. 1361–1368, Jun. 1998.

[57] N. K. Jha, P. S. Reddy, and V. R. Rao, “A New Drain Voltage Enhanced NBTI Degradation Mechanism,” in *Reliability Physics Symposium, 43rd IEEE*, 2005, pp. 524–528.

[58] W. McMahon, H. A. Birdsall, G. R. Johnson, and C. T. Camilli, “Degradation Studies of Polyethylene Terephthalate,” *Journal of Chemical Engineering Data*, vol. 4, pp. 57–79, 1959.

[59] J. H. Wohlgemuth and S. Kurtz, “Reliability Testing Beyond Qualification as a Key Component in Photovoltaic’s Progress Toward Grid Parity,” in *IEEE International Reliability Physics Symposium*, 2011, no. February.

[60] W. J. Gambogi, “Comparative Performance of Backsheets for Photovoltaic Modules,” in *European Photovoltaic Solar Energy Conference and Exhibition, 25th*, 2010, pp. 4079–4083.

[61] K. Whitfield and A. Salomon, “Modeling based on Damp Heat Testing,” in *PV Module Reliability Workshop*, 2012.

[62] J. Strauch, “PV Module Arc Fault Modeling and Analysis,” in *PV Module Reliability Workshop*, 2011.

[63] S. Koch and D. Nieschalk, “Potential Induced Degradation Effects on Crystalline Silicon Cells with Various Antireflective Coatings,” *27th European Photovoltaic Solar Energy Conference and Exhibition*, no. September, 2012.

[64] D. H. Meakin, “Fraunhofer PV Module Durability Initiative,” 2013.

[65] G. Tamizhmani, “Testing the reliability and safety of photovoltaic modules : failure rates and temperature effects,” 2009.

[66] E. Maset, E. Sanchis-kilders, J. B. Ejea, A. Ferreres, J. Jordán, V. Esteve, P. Brosselard, X. Jordà, M. Vellvehi, and P. Godignon, “Accelerated Life Test for SiC Schottky Blocking Diodes in High-Temperature Environment,” *IEEE Transactions on Device and Materials Reliability*, vol. 9, no. 4, pp. 557–562, 2009.

[67] S. Somisetty, P. Ersland, X. Yang, and J. Barrett, “Reliability investigation and characterization of failure modes in Schottky diodes,” *Microelectronics Reliability*, vol. 46, no. 8, pp. 1254–1260, Aug. 2006.

[68] W. Nelson, *Introduction and Background, in Accelerated Testing: Statistical Models, Test Plans, and Data Analysis*. Hoboken, NJ, USA: John Wiley & Sons, Inc., 2008.

[69] D. Jordan, “PV System Quarterly Report,” 2011.

Contributors: Zach Campeau, Michael Anderson Ph.D., Ernest Hasselbrink, Ph.D., David Kavulak Ph.D., Yu-Chen Shen Ph.D., Ryan Lacerda, Akira Terao Ph.D., Sander Caldwell Ph.D., Zoe Defreitas, Lauren Leonard, Mark Mikofski Ph.D., Dave DeGraaff, Ph.D, Arief Budiman Ph.D.